

# Transmutation based Quantum Simulation for Non-unitary Dynamics

Shi Jin<sup>\*1</sup>, Chuwen Ma<sup>†2,3</sup>, and Enrique Zuazua<sup>‡4,5,6</sup>

<sup>1</sup>School of Mathematical Sciences, Institute of Natural Sciences, MOE-LSC, Shanghai Jiao Tong University, Shanghai, 200240, China

<sup>2</sup>School of Mathematical Sciences, Key Laboratory of MEA, Ministry of Education, East China Normal University, Shanghai 200241, China,

<sup>3</sup> Shanghai Key Laboratory of PMMP, East China Normal University, Shanghai 200241, China

<sup>4</sup>Chair for Dynamics, Control, Machine Learning and Numerics, Alexander von Humboldt-Professorship, Department of Mathematics, Friedrich-Alexander-Universität Erlangen-Nürnberg, 91058 Erlangen, Germany

<sup>5</sup>Chair of Computational Mathematics, Fundación Deusto, Av. de las Universidades, 24, 48007 Bilbao, Basque Country, Spain

<sup>6</sup>Departamento de Matemáticas, Universidad Autónoma de Madrid, 28049 Madrid, Spain

January 8, 2026

## Abstract

We present a quantum algorithm for simulating dissipative diffusion dynamics generated by positive semidefinite operators of the form  $A = L^\dagger L$ , a structure that arises naturally in standard discretizations of elliptic operators. Our main tool is the Kannai transform, which represents the diffusion semigroup  $e^{-TA}$  as a Gaussian-weighted superposition of unitary wave propagators. This representation leads to a linear-combination-of-unitaries implementation with a Gaussian tail and yields query complexity  $\tilde{\mathcal{O}}(\sqrt{\|A\|T} \log(1/\varepsilon))$ , up to standard dependence on state-preparation and output norms, improving the scaling in  $\|A\|$ ,  $T$ , and  $\varepsilon$  compared with generic Hamiltonian-simulation-based methods. We instantiate the method for the heat equation and biharmonic diffusion under non-periodic physical boundary conditions, and we further use it as a subroutine for constant-coefficient linear parabolic surrogates arising in entropy-penalization schemes for viscous Hamilton–Jacobi equations. In the long-time regime, the same framework yields a structured quantum linear solver for  $A\mathbf{x} = \mathbf{b}$  with  $A = L^\dagger L$ , achieving  $\tilde{\mathcal{O}}(\kappa^{3/2} \log^2(1/\varepsilon))$  queries and improving the condition-number dependence over standard quantum linear-system algorithms in this factorized setting.

---

<sup>\*</sup>shijin-m@sjtu.edu.cn

<sup>†</sup>cwma@math.ecnu.edu.cn

<sup>‡</sup>enrique.zuazua@fau.de

**Keywords:** Kannai transform, Linear-combination-of-unitaries, Optimal query complexity, Linear solver

## 1 Introduction

Dissipative partial differential equations (PDEs), such as the heat equation and more general parabolic systems, are fundamental models for diffusion, relaxation, and transport across science and engineering. In high-dimensional regimes, classical discretization-based solvers may become computationally prohibitive, motivating alternative paradigms. Quantum computers can represent high-dimensional vectors as amplitude-encoded quantum states and, in principle, yield speedups for certain linear-algebraic primitives [23, 44–46].

A core difficulty is that quantum hardware natively implements *unitary* time evolution, whereas diffusion is intrinsically *non-unitary*. This mismatch helps explain why Hamiltonian simulation—the simulation of Schrödinger dynamics—became an early and central target of quantum algorithms, leading to a mature toolkit with near-optimal complexity guarantees [2, 5–7, 11, 17, 29, 33, 39, 40]. Designing quantum algorithms for dissipative dynamics therefore requires representing a non-unitary semigroup in terms of unitary primitives while retaining favorable dependence on the final time and the target accuracy.

**Our approach.** We propose a quantum algorithm based on the classical *Kannai transformation* (also known as *transmutation* or *subordination*) [31, 47, 54]. For generators of the form

$$\mathcal{A} = \mathcal{L}^\dagger \mathcal{L} \succeq 0,$$

the Kannai representation expresses the diffusion semigroup  $e^{-t\mathcal{A}}$  as a Gaussian-weighted superposition of unitary wave propagators associated with  $\mathcal{L}$ . Algorithmically, we simulate the corresponding reversible dynamics and recover the diffusion solution by evaluating a Gaussian convolution in an auxiliary time variable.

This viewpoint is related to dilation-based *wrap-and-average* methods (e.g. Schrödingerization and its Fourier/contour variants), where the cost is governed by truncating an auxiliary kernel [1, 3, 26, 29, 30, 35, 51]. The key quantitative distinction is that exponentially decaying kernels typically require truncation radii  $R = \Theta(T \log(1/\varepsilon))$ , whereas the Gaussian Kannai kernel yields  $R = \Theta(\sqrt{T \log(1/\varepsilon)})$ , improving the  $\varepsilon$ -and- $T$ -dependence of the resulting algorithms.

**Related work.** Existing approaches to non-unitary simulation include: (i) discretize and solve via quantum linear system algorithms (QLSAs) [4, 8, 9, 13, 16, 28, 34, 52]; (ii) dilate to a unitary PDE and apply Hamiltonian simulation [26, 29, 30], with closely related variants such as LCHS [1, 3] and contour-based matrix decomposition (CMD) [51]; and (iii) treat non-unitary generators via block-encoding or Lindbladian techniques [17, 48]. Our method belongs to the wrap-and-average family but exploits the Gaussian tail of the Kannai kernel to sharpen the dependence on  $\varepsilon$  for the structured class  $\mathcal{A} = \mathcal{L}^\dagger \mathcal{L}$ .

**Problem setting and contributions.** We consider inhomogeneous linear evolution problems

$$\frac{du}{dt} = -\mathcal{A}u + f, \quad u(0, \cdot) = u_0, \tag{1.1}$$

where  $\mathcal{A} = \mathcal{L}^\dagger \mathcal{L}$  is self-adjoint and non-negative and  $f$  is a time-independent source. After spatial discretization, this yields a matrix  $A = L^\dagger L$ . We assume standard quantum access to the discretized operators via block-encodings and to the input data via state preparation (see Section 4).

Our main contributions are as follows.

- **Kannai-based quantum simulation of diffusion.** We combine the Gaussian decay of the Kannai kernel with high-order quadrature in the auxiliary variable, the linear-combination-of-unitaries (LCU) framework, and near-optimal Hamiltonian simulation to obtain a quantum algorithm for (1.1). The query complexity to a block-encoding of the Hermitian dilation Hamiltonian scales as

$$\tilde{\mathcal{O}}(u_r \sqrt{T \|A\| \log(1/\varepsilon)}),$$

where  $T$  is the final time,  $\varepsilon$  is the target precision, and  $u_r$  captures the relative size of the input and forcing. Up to polylogarithmic factors, this improves the dependence on  $\varepsilon$ ,  $T$ , and  $\|A\|$  compared with wrap-and-average methods based on exponentially decaying kernels.

- **PDE instantiations and boundary conditions.** We apply the framework to the heat equation and biharmonic diffusion, and show that Dirichlet and Neumann boundary conditions can be handled without changing the leading-order complexity under standard sparse discretizations on bounded domains.
- **A structured quantum linear solver from long-time dynamics.** In the strongly dissipative regime, we solve  $A\mathbf{x} = \mathbf{b}$  with  $A = L^\dagger L$  by running the dynamics to  $T = \Theta(\kappa \log(1/\varepsilon))$  and applying the Kannai-based simulator. This yields a quantum linear solver with query complexity

$$\tilde{\mathcal{O}}(\kappa^{3/2} \log^2(1/\varepsilon)),$$

improving the condition-number dependence over general-purpose QLSAs in this factorized setting.

- **Further transmutation constructions.** We collect additional transmutation-based reductions representing target dynamics as superpositions of reversible evolutions, including algorithms for second-order-in-time models (e.g. Euler–Poisson–Darboux via spherical means) and an alternative reduction from the heat equation to unitary transport via transport–heat averaging.

**Organization.** Section 2 reviews transmutation and rewrites it as a first-order Hamiltonian system suitable for quantum simulation. Section 3 presents discretization, Gaussian quadrature, and error analysis. Section 4 gives the quantum implementation and query bounds, and Section 5 illustrates them on heat, viscous Hamilton–Jacobi, and biharmonic diffusion. Section 6 addresses the long-time regime and the induced linear solver. Section 7 collects additional transmutation-based constructions. Section 8 presents numerical experiments that validate the correctness of the Kannai-transform-based LCU method. Conclusions are in Section 9.

**Notation.** For  $j \in [N]$ ,  $|j\rangle \in \mathbb{C}^N$  denotes the  $j$ th computational basis vector. We write  $\tilde{O}(\cdot)$  to suppress polylogarithmic factors, and  $f \lesssim g$  to denote  $f \leq Cg$  with a constant  $C > 0$  independent of sensitive parameters. All logarithms are natural.

## 2 Transmutation and unitary superpositions

Transmutation methods provide a classical route for reducing a given evolution problem to another one whose analysis is already available. Typical objectives include replacing equations with singular coefficients by regular ones, removing small parameters, or relating second-order and first-order evolutions. We refer to [10, 20, 32, 37, 38, 49] for representative developments. In this section we use transmutation techniques to express a target non-unitary dynamics as a superposition of unitary evolutions. This structure is particularly suitable for quantum algorithm design.

### 2.1 Kannai transformation for the linear system

We consider the setting in which the spatial operator admits the factorization

$$\mathcal{A} = \mathcal{L}^\dagger \mathcal{L}, \quad (2.1)$$

together with boundary conditions that make  $\mathcal{A}$  nonnegative and self-adjoint. A prototypical example is  $\mathcal{L} = -\nabla$  as a map from  $H_0^1(\Omega)$  to  $L^2(\Omega)$ . In this case  $\mathcal{A} = -\Delta_x$  with homogeneous Dirichlet boundary conditions. We study the linear system with a time-independent source term

$$\frac{du(t, x)}{dt} = -\mathcal{A}u(t, x) + f(x), \quad u(0, x) = u_0(x). \quad (2.2)$$

Kannai [31] shows that one can represent  $u$  via a transmutation operator acting only on the time variable:

$$u(t, x) = (\mathcal{H}w)(t, x) = \int_{\mathbb{R}} K(t, s) w(s, x) ds. \quad (2.3)$$

The kernel is Gaussian,

$$K(t, s) = \frac{1}{\sqrt{4\pi t}} e^{-s^2/(4t)}. \quad (2.4)$$

The auxiliary function  $w$  solves the inhomogeneous wave-type equation

$$w_{ss}(s, x) = -\mathcal{A}w(s, x) + f(x), \quad w(0, x) = u_0(x), \quad w_s(0, x) = 0. \quad (2.5)$$

### 2.2 Unitary embedding via first-order factorization

To reveal the unitary dynamics underlying (2.5), we recast the second-order equation as a first-order system. Introduce an auxiliary variable  $v$  by

$$\frac{d}{ds} v(s, x) = -\mathcal{L}w(s, x), \quad v(0, x) = 0.$$

Define the augmented state, the embedded source term, and the block operator by

$$\psi(s, x) = [w(s, x) \ v(s, x)]^\top, \quad \tilde{f}(x) = [f(x) \ 0]^\top, \quad \tilde{\mathcal{L}} = \begin{bmatrix} 0 & \mathcal{L}^\dagger \\ -\mathcal{L} & 0 \end{bmatrix}. \quad (2.6)$$

A direct calculation shows that  $\psi$  satisfies the inhomogeneous first-order system

$$\frac{d}{ds}\psi(s, x) = \tilde{\mathcal{L}}\psi(s, x) + s\tilde{\mathbf{f}}(x), \quad \psi(0, x) = \psi_0(x), \quad (2.7)$$

where  $\psi_0(x) = [u_0(x), 0]^\top$ . By Duhamel's principle, (2.7) admits the variation-of-constants formula

$$\psi(s, x) = \mathcal{U}(s)\psi_0(x) + \int_0^s \sigma \mathcal{U}(s-\sigma)\tilde{\mathbf{f}}(x) d\sigma, \quad \mathcal{U}(s) = \exp(\tilde{\mathcal{L}}s). \quad (2.8)$$

The operator  $\tilde{\mathcal{L}}$  is skew-adjoint under the boundary conditions inherited from  $\mathcal{L}$ . Consequently, the homogeneous evolution  $\mathcal{U}(s)$  is unitary. This unitary structure will be central in our quantum constructions.

The next lemma makes explicit that the transmutation formula expresses  $u$  as an integral superposition of the unitary dynamics generated by  $\tilde{\mathcal{L}}$ .

**Lemma 2.1.** *Let  $\mathcal{A} = \mathcal{L}^\dagger \mathcal{L}$  be a nonnegative self-adjoint operator independent of time. Assume that  $u$  and  $w$  satisfy (2.2) and (2.5), respectively. Let  $\mathcal{H}$  be the transmutation operator in (2.3) with kernel (2.4). Then*

$$u(t, x) = \Pi_1 \left( \int_{\mathbb{R}} K(t, s) \mathcal{U}(s) \psi_0(x) ds + \int_{\mathbb{R}} K(t, s) \int_0^s \sigma \mathcal{U}(s-\sigma) \tilde{\mathbf{f}}(x) d\sigma ds \right), \quad (2.9)$$

where  $\Pi_1$  denotes the projection onto the first component,  $\psi_0$  and  $\tilde{\mathbf{f}}$  are defined in (2.6), and  $\mathcal{U}(s)$  is given by (2.8).

### 3 Numerical discretization

In this section we construct a fully discrete formulation of the proposed representation. We discretize the first-order system in space to obtain a semi-discrete unitary evolution, then approximate the resulting Gaussian integrals by quadrature and derive error bounds.

#### 3.1 Spatial discretization of the first-order system

To discretize (2.7) in space, we introduce a matrix  $L \in \mathbb{C}^{N \times N}$  arising from an appropriate spatial discretization of the differential operator  $\mathcal{L}$ . Let  $\mathbf{w}_h(s), \mathbf{v}_h(s) \in \mathbb{C}^N$  denote the semi-discrete approximations of  $w(s, \cdot)$  and  $v(s, \cdot)$ , and let  $\mathbf{f}_h \in \mathbb{C}^N$  be the discrete source term. Define the stacked state vector and forcing vector by

$$\psi_h(s) = \begin{bmatrix} \mathbf{w}_h(s) \\ \mathbf{v}_h(s) \end{bmatrix} \in \mathbb{C}^{2N}, \quad \psi_0 = \begin{bmatrix} \mathbf{u}_0 \\ \mathbf{0} \end{bmatrix} \in \mathbb{C}^{2N}, \quad \mathbf{b} = \begin{bmatrix} \mathbf{f}_h \\ \mathbf{0} \end{bmatrix} \in \mathbb{C}^{2N}, \quad (3.1)$$

where  $\mathbf{u}_0$  denotes the discrete initial data. The semi-discrete system can be written as

$$\frac{d}{ds}\psi_h(s) = \tilde{L}\psi_h(s) + s\mathbf{b} =: -iH\psi_h(s) + s\mathbf{b}, \quad (3.2)$$

with the anti-Hermitian matrix  $\tilde{L}$  and its Hermitian counterpart  $H$  given by

$$\tilde{L} = |0\rangle\langle 1| \otimes L^\dagger - |1\rangle\langle 0| \otimes L \in \mathbb{C}^{2N \times 2N}, \quad H = i\tilde{L}. \quad (3.3)$$

Hence the homogeneous propagator  $U(s) := \exp(-iHs)$  is unitary. By Duhamel's principle, the solution of (3.2) admits the representation

$$\psi_h(s) = U(s)\psi_0 + \left( \int_0^s (s-\sigma) U(\sigma) d\sigma \right) \mathbf{b}. \quad (3.4)$$

Based on (3.4), we define the discrete target at time  $T > 0$  by the Kannai Gaussian integral

$$\begin{aligned} \mathbf{u}_f^{\text{disc}}(T) &:= \int_{\mathbb{R}} K(T, s) \psi_h(s) ds \\ &= \left( \int_{\mathbb{R}} \kappa_T(s) U(s) ds \right) \psi_0 + \left( \int_{\mathbb{R}} \kappa_T(s) \int_0^s (s-\sigma) U(\sigma) d\sigma ds \right) \mathbf{b} \end{aligned} \quad (3.5)$$

with

$$\kappa_T(s) = K(T, s) = (4\pi T)^{-1/2} e^{-s^2/(4T)}. \quad (3.6)$$

We also introduce the Gaussian tail function

$$\Phi_T(a) := \frac{1}{\sqrt{4\pi T}} \int_a^\infty e^{-s^2/(4T)} ds = \frac{1}{2} \operatorname{erfc}\left(\frac{a}{2\sqrt{T}}\right).$$

Since  $U(s)$  is unitary and  $\kappa_T$  is integrable on  $\mathbb{R}$ , all integrals above are absolutely convergent, and Fubini's theorem applies. Exchanging the order of integration reduces the nested term in (3.5) to a one-dimensional integral of the form. More precisely, one obtains the representation

$$\mathbf{u}_f^{\text{disc}}(T) = \left( \int_{\mathbb{R}} \kappa_T(s) U(s) ds \right) \psi_0 + \left( \int_{\mathbb{R}} \Lambda_T(\sigma) U(\sigma) d\sigma \right) \mathbf{b}, \quad (3.7)$$

where the scalar kernel  $\Lambda_T$  is given by

$$\Lambda_T(\sigma) = \begin{cases} \frac{1}{\sqrt{4\pi T}} \int_\sigma^\infty e^{-s^2/(4T)} (s-\sigma) ds = \sqrt{\frac{T}{\pi}} e^{-\sigma^2/(4T)} - \sigma \Phi_T(\sigma), & \sigma \geq 0, \\ \frac{1}{\sqrt{4\pi T}} \int_{-\infty}^\sigma e^{-s^2/(4T)} (s-\sigma) ds = -\sqrt{\frac{T}{\pi}} e^{-\sigma^2/(4T)} - \sigma \Phi_T(-\sigma), & \sigma < 0. \end{cases} \quad (3.8)$$

## 3.2 Numerical integration

For numerical implementation, we truncate the infinite integration domain to a finite interval  $[-R, R]$  with  $R > 0$ . We partition  $[-R, R]$  into uniform panels of length  $h_1 > 0$ . Let  $M_R := R/h_1$  and assume that  $M_R$  is an integer. The panels are indexed by  $m = -M_R, \dots, M_R - 1$  and given by  $[mh_1, (m+1)h_1]$ . On each panel we apply a  $Q$ -point Gauss–Legendre rule. Let  $\{x_q, \omega_q\}_{q=1}^Q$  be the standard Gauss–Legendre nodes and weights on  $[-1, 1]$ . The corresponding nodes and rescaled weights on  $[mh_1, (m+1)h_1]$  are

$$s_{q,m} = \frac{h_1}{2} x_q + \frac{2m+1}{2} h_1, \quad w_{q,m} = \frac{h_1}{2} \omega_q, \quad q = 1, \dots, Q. \quad (3.9)$$

We assume that the kernel values can be precomputed offline to high precision. More precisely, we use approximations  $\kappa_T^a$  and  $\Lambda_T^a$  satisfying

$$|\kappa_T^a(s) - \kappa_T(s)| \leq \delta_{\text{off}} |\kappa_T(s)|, \quad \forall s \in \mathbb{R}, \quad (3.10)$$

and

$$|\Lambda_T^a(s) - \Lambda_T(s)| \leq \delta_{\text{off}} |\Lambda_T(s)|, \quad \forall s \in \mathbb{R}. \quad (3.11)$$

With these ingredients, the quadrature approximations of the two integrals in (3.7) lead to the discrete representation

$$\mathbf{u}_f^{\text{disc}}(T) \approx \mathbf{u}_f^h(T) = \sum_{m=-M_R}^{M_R-1} \sum_{q=1}^Q \left( c_{q,m} U(s_{q,m}) \boldsymbol{\psi}_0 + d_{q,m} U(s_{q,m}) \mathbf{b} \right), \quad (3.12)$$

where

$$c_{q,m} = w_{q,m} \kappa_T^a(s_{q,m}), \quad d_{q,m} = w_{q,m} \Lambda_T^a(s_{q,m}). \quad (3.13)$$

**Remark 3.1.** The offline precomputation of  $\kappa_T$  and  $\Lambda_T$  removes the need to evaluate nested integrals during the online stage. Both contributions in (3.7) reduce to one-dimensional weighted sums over quadrature nodes. Alternative quadrature rules such as the trapezoidal rule or Monte Carlo sampling can be incorporated analogously. The choice of quadrature affects the required coefficient precision but does not change the final query complexity of the quantum procedure, since coefficient precision enters only polylogarithmically in the relevant qubit complexity.

### 3.3 Error analysis for the quadrature discretization

We estimate the error of the fully discrete quadrature scheme for approximating  $\mathbf{u}_f^{\text{disc}}(T)$  by  $\mathbf{u}_f^h(T)$ . We bound

$$\mathcal{E} = \left\| \mathbf{u}_f^h(T) - \mathbf{u}_f^{\text{disc}}(T) \right\|.$$

The error consists of three contributions: truncation on  $[-R, R]$ , quadrature discretization on each panel, and offline kernel approximation. We state the final bounds here and defer the proofs to Appendix A.

**Theorem 3.1.** *Assume the hypotheses of Lemmas A.1 and A.4 hold. Let  $\mathbf{u}_f^h(T)$  denote the truncated quadrature approximation in (3.12) and let  $\mathbf{u}_f^{\text{disc}}(T)$  be the target integral representation in (3.7). Then, for any  $\epsilon \in (0, 1)$ , there exist parameters  $R > 0$ , an integer  $Q \geq 1$ , a panel size  $h_1 > 0$ , and an offline-kernel accuracy  $\delta_{\text{off}} > 0$  such that*

$$\mathcal{E} \leq \epsilon (\|\boldsymbol{\psi}_0\| + T\|\mathbf{b}\|).$$

Moreover, the total coefficient magnitudes satisfy

$$\sum_{m,q} |c_{q,m}| \leq 1 + \epsilon, \quad \sum_{m,q} |d_{q,m}| \leq (1 + \epsilon)T + \epsilon.$$

In particular, the above bounds hold under the explicit choices

$$R = 2\sqrt{T} \sqrt{\log\left(\frac{8}{\epsilon}\right)} = \mathcal{O}(\sqrt{T \log(1/\epsilon)}), \quad (3.14)$$

and

$$Q \geq \left\lceil \log_2 \left( \frac{8R}{\epsilon\sqrt{T}} \right) \right\rceil = \mathcal{O}(\log(1/\epsilon)), \quad h_1 \leq \frac{\sqrt{T}}{e(\|H\| + \frac{1}{\sqrt{2T}})}, \quad \delta_{\text{off}} \leq \frac{\epsilon}{4}. \quad (3.15)$$

*Proof.* The proof is finished by inserting the parameter choices (3.14) and (3.15) into the bounds of Lemma A.4.  $\square$

## 4 Quantum implementation and query complexity

In this section we present the quantum implementation of our method for the inhomogeneous system in (2.2) and derive the resulting query complexity bounds.

For the quantum implementation we flatten the double index  $(q, m)$  into a single index  $j \in \{0, \dots, M-1\}$ , where  $M = QM_R$ . We write

$$c_j := c_{q,m}, \quad d_j := d_{q,m}, \quad s_j := s_{q,m}.$$

Since the same quadrature nodes are used for both sums, the discrete representation (3.12) becomes

$$\mathbf{u}_f^h = \sum_{j=0}^{M-1} (c_j U(s_j) \psi_0 + d_j U(s_j) \mathbf{b}), \quad (4.1)$$

where  $U(s) = \exp(-iHs)$  and  $H$  is given in (3.3).

### 4.1 Block-encoding of the Hamiltonians

We work in the standard sparse-query/block-encoding model [11, 18, 36]. Assume access to an  $(\alpha_L, a_L, 0)$ -block-encoding of  $L$ , namely a unitary  $U_L$  such that

$$(\langle 0^{a_L} | \otimes I_N) U_L (|0^{a_L}\rangle \otimes I_N) = \frac{L}{\alpha_L}, \quad \alpha_L \geq \|L\|. \quad (4.2)$$

Then  $U_L^\dagger$  block-encodes  $L^\dagger$  with the same parameters.

Define the Hermitian dilation

$$\tilde{H}_0 := |0\rangle\langle 1| \otimes L^\dagger + |1\rangle\langle 0| \otimes L.$$

Using one additional ‘‘position’’ qubit and  $U_L, U_L^\dagger$ , one can construct a unitary  $W_{H_0}$  acting on  $a_H := a_L + 1$  ancillas and the  $2N$ -dimensional signal space such that

$$(\langle 0^{a_H} | \otimes I_{2N}) W_{H_0} (|0^{a_H}\rangle \otimes I_{2N}) = \frac{\tilde{H}_0}{\alpha_L}. \quad (4.3)$$

With  $P := |0\rangle\langle 0| + i|1\rangle\langle 1|$ , one has  $H = (P \otimes I_N) \tilde{H}_0 (P^\dagger \otimes I_N)$ . Define

$$\text{HAM}_H := (I_{a_H} \otimes P \otimes I_N) W_{H_0} (I_{a_H} \otimes P^\dagger \otimes I_N). \quad (4.4)$$

Then  $\text{HAM}_H$  is an  $(\alpha_H, a_H, 0)$ -block-encoding of  $H$  with  $\alpha_H = \Theta(\alpha_L)$ , and each call to  $\text{HAM}_H$  uses  $\mathcal{O}(1)$  queries to  $U_L$  and  $U_L^\dagger$ .

Let  $s_{\max} := \max_j |s_j| \leq R$  and set  $\gamma_j := s_j/s_{\max} \in [-1, 1]$ . Using reversible arithmetic, we implement scalar-preparation oracles  $O_{\gamma, L}$  and  $O_{\gamma, R}$  such that, conditioned on  $|j\rangle$ , they prepare amplitudes and phases for  $\gamma_j$ :

$$\begin{aligned} O_{\gamma, L} : |j\rangle |0\rangle_\gamma &\mapsto |j\rangle \left( \sqrt{|\gamma_j|} |0\rangle_\gamma + \sqrt{1 - |\gamma_j|} |1\rangle_\gamma \right), \\ O_{\gamma, R} : |j\rangle |0\rangle_\gamma &\mapsto |j\rangle \left( e^{i\theta_j^{(\gamma)}} \sqrt{|\gamma_j|} |0\rangle_\gamma + \sqrt{1 - |\gamma_j|} |1\rangle_\gamma \right). \end{aligned} \quad (4.5)$$

The resulting overhead is polylogarithmic in the target precision. With these, define the unitary  $\text{HAM}_{H_s}$  by

$$\begin{aligned} \text{HAM}_{H_s} := I_M \otimes & \left( (O_{\gamma, \text{L}}^\dagger \otimes I_{a_H} \otimes I_{2N}) \right. \\ & \left. \cdot (|0\rangle\langle 0|_\gamma \otimes \text{HAM}_H + |1\rangle\langle 1|_\gamma \otimes I_{a_H} \otimes I_{2N}) \cdot (O_{\gamma, \text{R}} \otimes I_{a_H} \otimes I_{2N}) \right). \end{aligned} \quad (4.6)$$

Then, on the joint index–signal space,

$$(I_M \otimes \langle 0|_\gamma \langle 0^{a_H} | \otimes I_{2N}) \text{HAM}_{H_s} (I_M \otimes |0\rangle_\gamma |0^{a_H}\rangle \otimes I_{2N}) = \sum_{j=0}^{M-1} |j\rangle\langle j| \otimes \frac{s_j H}{\alpha_H s_{\max}}. \quad (4.7)$$

Hence  $\text{HAM}_{H_s}$  is an  $(\alpha_H s_{\max}, a_H + 1, 0)$ -block-encoding of the block-diagonal Hamiltonian

$$H_S := \sum_{j=0}^{M-1} s_j |j\rangle\langle j| \otimes H, \quad (4.8)$$

where the index register is treated as part of the signal space and not counted as ancillas.

## 4.2 Implementation of unitary time evolution

Using the above  $(\alpha_H s_{\max}, a_H + 1, 0)$ -block-encoding of  $H_S$ , we aim to implement

$$e^{-iH_S} = \sum_{j=0}^{M-1} |j\rangle\langle j| \otimes e^{-iH s_j} = \sum_{j=0}^{M-1} |j\rangle\langle j| \otimes U(s_j).$$

Applying a QSVT-based Hamiltonian simulation routine to the normalized block-encoding  $H_S/(\alpha_H s_{\max})$  [1, 42], we obtain a unitary SEL acting on an additional ancilla register of size  $a_{\text{QSVT}}$  such that

$$(I_M \otimes \langle 0^{a_{\text{tot}}} | \otimes I_{2N}) \text{SEL} (I_M \otimes |0^{a_{\text{tot}}}\rangle \otimes I_{2N}) = \sum_{j=0}^{M-1} |j\rangle\langle j| \otimes U_j^a, \quad (4.9)$$

where  $a_{\text{tot}} := a_H + 1 + a_{\text{QSVT}}$  and

$$\|U_j^a - U(s_j)\| \leq \delta_1 \quad \text{for all } j \in \{0, \dots, M-1\}.$$

By [1, Corollary 16], constructing SEL uses the block-encoding oracle for  $H_S$  a total of

$$\tilde{\mathcal{O}}\left(\alpha_H s_{\max} + \log(1/\delta_1)\right) \quad (4.10)$$

queries, up to polylogarithmic factors in the relevant precision parameters.

## 4.3 The LCU implementation of the discrete representation

We assume access to state-preparation oracles

$$O_\psi : |0\rangle \mapsto |\psi_0\rangle, \quad O_b : |0\rangle \mapsto |\mathbf{b}\rangle.$$

We also assume access to standard coefficient oracles  $O_{c, \text{L}}, O_{c, \text{R}}$  and  $O_{d, \text{L}}, O_{d, \text{R}}$  that, conditioned on  $j$ , prepare amplitudes proportional to  $|c_j|$  and  $|d_j|$  and encode the phases  $e^{i\theta_j^{(c)}}$  and  $e^{i\theta_j^{(d)}}$  required by the linear combination of unitary (LCU) framework [12].

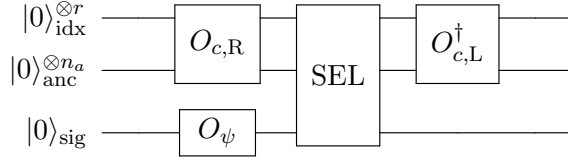


Fig. 1: Quantum circuit for the homogeneous term.

Write  $c_j = |c_j|e^{i\theta_j^{(c)}}$  and  $d_j = |d_j|e^{i\theta_j^{(d)}}$ , and set

$$\alpha_c := \sum_{j=0}^{M-1} |c_j|, \quad \alpha_d := \sum_{j=0}^{M-1} |d_j|. \quad (4.11)$$

Using (4.9), the homogeneous contribution in (4.1) admits the LCU block-encoding

$$\mathcal{W}_{\text{hom}}^a = (O_{c,\text{L}}^\dagger \otimes I) \text{SEL} (O_{c,\text{R}} \otimes O_\psi), \quad (\langle 0 | \otimes I) \mathcal{W}_{\text{hom}}^a (|0\rangle \otimes I) = \frac{1}{\alpha_c} \sum_{j=0}^{M-1} c_j U_j^a. \quad (4.12)$$

The inhomogeneous contribution is realized analogously by

$$\mathcal{W}_{\text{inh}}^a = (O_{d,\text{L}}^\dagger \otimes I) \text{SEL} (O_{d,\text{R}} \otimes O_b), \quad (\langle 0 | \otimes I) \mathcal{W}_{\text{inh}}^a (|0\rangle \otimes I) = \frac{1}{\alpha_d} \sum_{j=0}^{M-1} d_j U_j^a. \quad (4.13)$$

Summarizing, there exist an integer  $n_a$  and a unitary  $V_0$  acting on the index register,  $n_a$  ancilla qubits, and the  $2N$ -dimensional signal register such that

$$|0^{\otimes r}\rangle_{\text{idx}} |0^{\otimes n_a}\rangle_{\text{anc}} |0\rangle_{\text{sig}} \xrightarrow{V_0} \frac{1}{\eta_0} |0^{\otimes r}\rangle_{\text{idx}} |0^{\otimes n_a}\rangle_{\text{anc}} \otimes \mathbf{u}_f^a + |\perp\rangle. \quad (4.14)$$

For brevity we omit additional workspace qubits used by reversible arithmetic, which are uncomputed at the end. Here the state  $|\perp\rangle$  has index–ancilla part orthogonal to  $|0^{\otimes r}\rangle_{\text{idx}} |0^{\otimes n_a}\rangle_{\text{anc}}$ , we use the embedding  $\psi_0 = |0\rangle \otimes \mathbf{u}_0$ , and

$$\mathbf{u}_f^a = \sum_{j=0}^{M-1} (c_j U_j^a \psi_0 + d_j U_j^a \mathbf{b}), \quad \eta_0 = \Theta(\alpha_c \|\mathbf{u}_0\| + \alpha_d \|\mathbf{b}\|). \quad (4.15)$$

For clarity, we focus on the homogeneous case and present the overall quantum circuit that implements the corresponding LCU construction (see Fig. 1). The circuit starts from  $|0^{\otimes r}\rangle_{\text{idx}} |0^{\otimes n_a}\rangle_{\text{anc}} |0\rangle_{\text{sig}}$ , where  $r = \lceil \log_2 M \rceil$ . The signal register is then initialized by the state-preparation oracle  $O_\psi$  so that  $O_\psi |0\rangle_{\text{sig}} = |\psi_0\rangle$ , while the index and ancilla registers are prepared in the all-zero state. The ancilla register in Fig. 1 collects all ancillas used by the coefficient-preparation oracles and by SEL; in particular it includes the  $a_{\text{tot}}$  ancillas of SEL.

#### 4.4 Query complexity

The circuit  $V_0$  prepares an unnormalized state  $\mathbf{u}_f^a$  in the  $|0^{\otimes n_a}\rangle$ -ancilla branch with prefactor  $1/\eta_0$ . Consequently, postselecting the ancillas on  $|0^{\otimes n_a}\rangle$  succeeds with probability  $\|\mathbf{u}_f^a\|^2/\eta_0^2$ . Let  $\mathbf{u}_h(T)$  denote the first component of  $\mathbf{u}_f(T)$ . Equivalently,  $\mathbf{u}_h(T)$  is obtained by postselecting

the position qubit on  $|0\rangle$ . Conditioned on the success event, this projection yields  $\mathbf{u}_h(T)$  with probability  $\|\mathbf{u}_h(T)\|^2/\|\mathbf{u}_f(T)\|^2$ . Applying oblivious amplitude amplification and then performing the projection, the repetition factor satisfies

$$g = \mathcal{O}\left(\frac{\eta_0}{\|\mathbf{u}_h(T)\|}\right) = \mathcal{O}\left(\frac{\alpha_c\|\mathbf{u}_0\| + \alpha_d\|\mathbf{b}\|}{\|\mathbf{u}_h(T)\|}\right). \quad (4.16)$$

Define

$$u_r := \frac{\|\mathbf{u}_0\| + T\|\mathbf{b}\|}{\|\mathbf{u}_h(T)\|}. \quad (4.17)$$

The resulting query complexity bounds are stated in Theorem 4.1.

**Theorem 4.1.** *Consider the linear equation in (2.2) with  $\mathcal{A} = \mathcal{L}^\top \mathcal{L}$  self-adjoint. Let  $L$  be the matrix obtained from the spatial discretization of  $\mathcal{L}$ . There exists a quantum algorithm that prepares an  $\varepsilon$ -approximation of the normalized solution state  $|\mathbf{u}_h(T)\rangle$  with  $\Omega(1)$  success probability and a success flag. Moreover, the total query complexity to the block-encoding oracle for  $H$  is*

$$\tilde{\mathcal{O}}\left(u_r\left(\|L\|\sqrt{T \log \frac{u_r}{\varepsilon}} + \log \frac{u_r}{\varepsilon}\right)\right),$$

and the number of calls to the state-preparation oracles  $O_\psi$  and  $O_b$  is  $\mathcal{O}(u_r)$ .

The above guarantees hold under the following default choices of auxiliary parameters.

**Table 1.** Default discretization choices used in the proof.

Parameter	Meaning	Default choice
$R$	truncation radius in $s$	$R = \sqrt{T \log\left(\frac{8u_r}{\varepsilon}\right)}$
$h_1$	panel length in $s$ (step size)	$h_1 = \frac{\sqrt{T}}{e(\ L\  + 1/\sqrt{2T})}$
$Q$	reference Gauss points per panel	$Q = \mathcal{O}\left(\log\left(\frac{8u_r}{\varepsilon}\right)\right)$
$\delta_{\text{off}}$	offline approximation error in (3.10) and (3.11)	$\delta_{\text{off}} = \frac{\varepsilon}{32u_r}$

*Proof.* Let  $\mathbf{u}_f^{\text{disc}}$  be the fully discrete vector in (3.7), let  $\mathbf{u}_f^h$  be the corresponding truncated quadrature target in (3.12), and let  $\mathbf{u}_f^a$  be the unnormalized vector produced by the quantum circuit in (4.15). For any nonzero vectors  $\mathbf{x}$  and  $\mathbf{y}$ ,  $\left\|\frac{\mathbf{x}}{\|\mathbf{x}\|} - \frac{\mathbf{y}}{\|\mathbf{y}\|}\right\| \leq \frac{2\|\mathbf{x} - \mathbf{y}\|}{\|\mathbf{x}\|}$ . Applying this with  $\mathbf{x} = \mathbf{u}_f^{\text{disc}}$  and  $\mathbf{y} = \mathbf{u}_f^a$  yields

$$\|\mathbf{u}_f^a\rangle - |\mathbf{u}_f^{\text{disc}}\rangle\| \leq \frac{2\|\mathbf{u}_f^{\text{disc}} - \mathbf{u}_f^h\|}{\|\mathbf{u}_f^{\text{disc}}\|} + \frac{2\|\mathbf{u}_f^h - \mathbf{u}_f^a\|}{\|\mathbf{u}_f^{\text{disc}}\|}. \quad (4.18)$$

**Step 1: Discretization error.** Choose the discretization parameters  $(R, h_1, Q, \delta_{\text{off}})$  as in Table 1, obtained by applying Theorem 3.1 with target accuracy  $\varepsilon/(8u_r)$ . Then

$$\|\mathbf{u}_f^{\text{disc}} - \mathbf{u}_f^h\| \leq \frac{\varepsilon}{8} \|\mathbf{u}_f^{\text{disc}}\|, \quad \alpha_c = \mathcal{O}(1), \quad \alpha_d = \mathcal{O}(T),$$

so the first term in (4.18) is at most  $\varepsilon/4$ .

**Step 2: Error from imperfect implementation of unitaries.** Let  $U(s) = e^{-iHs}$  and let  $U_j^a$  be the unitaries implemented by the selector SEL, satisfying  $\|U_j^a - U(s_j)\| \leq \delta_1$  for all  $j$  as in (4.9). Using the LCU representations of  $\mathbf{u}_f^h$  and  $\mathbf{u}_f^a$  yields

$$\begin{aligned} \|\mathbf{u}_f^h - \mathbf{u}_f^a\| &= \left\| \sum_{j=0}^{M-1} c_j (U(s_j) - U_j^a) \psi_0 + \sum_{j=0}^{M-1} d_j (U(s_j) - U_j^a) \mathbf{b} \right\| \\ &\leq \delta_1 (\alpha_c \|\psi_0\| + \alpha_d \|\mathbf{b}\|) = \delta_1 u_r \|\mathbf{u}_h(T)\|. \end{aligned} \quad (4.19)$$

Set

$$\delta_1 := \frac{\varepsilon}{8u_r}. \quad (4.20)$$

Using  $\|\mathbf{u}_h(T)\| \leq \|\mathbf{u}_f^{\text{disc}}\|$ , the second term in (4.18) is at most  $\varepsilon/4$ .

Combining the two steps gives

$$\|\langle \mathbf{u}_f^a \rangle - \langle \mathbf{u}_f^{\text{disc}} \rangle\| \leq \frac{\varepsilon}{2},$$

hence in particular an  $\varepsilon$ -approximation.

**Step 3: Query complexity.** Each invocation of SEL uses

$$\tilde{\mathcal{O}}\left(\alpha_H s_{\max} + \log \frac{1}{\delta_1}\right) = \tilde{\mathcal{O}}\left(\|L\| R + \log \frac{u_r}{\varepsilon}\right)$$

queries to the block-encoding of  $H$ , by (4.10) and (4.20). With the parameter choices in Table 1, one has  $R = \Theta(\sqrt{T \log(u_r/\varepsilon)})$ . Postselecting the position qubit yields a state proportional to  $|\mathbf{u}_h(T)\rangle$ , and the repetition factor is  $g = \mathcal{O}(u_r)$  by (4.16). Multiplying by  $g$  gives the stated total query complexity. The number of calls to  $O_\psi$  and  $O_b$  is also  $\mathcal{O}(u_r)$  since each attempt invokes them  $\mathcal{O}(1)$  times.  $\square$

**Remark 4.1.** Theorem 4.1 yields only polylogarithmic dependence on the target accuracy  $\varepsilon$ . Many quantum constructions for non-unitary linear dynamics approximate the propagator by a truncated unitary superposition

$$\mathcal{S}(T, 0)u_0 \approx \int_{-R}^R K(s) e^{-iHs} u_0 \, ds, \quad 2 \int_R^\infty |K(s)| \, ds \leq \varepsilon,$$

for which the dominant matrix-query cost is typically proportional to  $R$  up to polylogarithmic factors. In our case, the Kannai kernel is Gaussian, giving

$$R = \Theta(\sqrt{T \log(1/\varepsilon)}),$$

and hence the dominant term in the query bound is  $\tilde{\mathcal{O}}(u_r \|L\| \sqrt{T \log(1/\varepsilon)})$ . Moreover, since  $\mathcal{A} = \mathcal{L}^\dagger \mathcal{L}$  we have  $A = L^\dagger L$  and thus  $\|L\| = \|A\|^{1/2}$ , so the bound exhibits a square-root dependence on  $\|A\|$  rather than a linear one, improving upon [1, 27, 41]. Fig. 2 illustrates the truncation behavior of the corresponding kernels. In particular, our improved dependence can be summarized as

$$\tilde{\mathcal{O}}(\sqrt{\alpha_A T \log(1/\varepsilon)}),$$

as reported in Table 2 for the homogeneous setting.

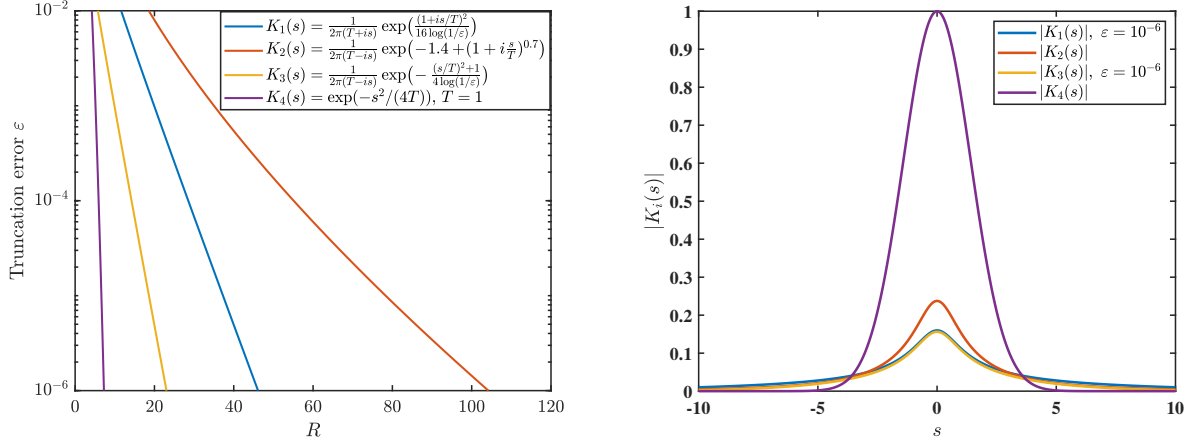


Fig. 2: Kernel truncation behaviour for several unitary-superposition representations. **Left:** truncation error  $\varepsilon(R) := 2 \int_R^\infty |K_i(s)| ds$  as a function of the truncation length  $R$  (logarithmic scale in  $\varepsilon$ ). **Right:** kernel magnitudes  $|K_i(s)|$  on  $s \in [-10, 10]$  for a fixed target precision  $\varepsilon = 10^{-6}$  and  $T = 1$ .

Table 2: Query complexities for homogeneous linear ODEs  $d\mathbf{u}/dt = A\mathbf{u}$  with time-independent generator  $A = L^\dagger L$ . Here  $T > 0$  is the final time,  $\alpha_A := \|A\|$ ,  $u_r := \|\mathbf{u}_0\|/\|\mathbf{u}(T)\|$ , and  $\varepsilon \in (0, 1)$  is the target precision. The parameter  $\beta \in (0, 1)$ .

Method	Kernel $K(s)$	Truncation length	Matrix queries
Optimal Schrödingerization [27]	$\frac{\exp\left(\frac{(1+is/T)^2}{16\log(1/\varepsilon)}\right)}{2\pi(T+is)}$	$\mathcal{O}\left(T \log \frac{1}{\varepsilon}\right)$	$\tilde{\mathcal{O}}\left(u_r \alpha_A T \log \frac{1}{\varepsilon}\right)$
Improved LCHS [1]	$\frac{\exp\left(2^\beta - (1+is/T)^\beta\right)}{2\pi(T-is)}$	$\mathcal{O}\left(T \log^{\frac{1}{\beta}} \frac{1}{\varepsilon}\right)$	$\tilde{\mathcal{O}}\left(u_r \alpha_A T \log^{\frac{1}{\beta}} \frac{1}{\varepsilon}\right)$
Optimal LCHS [41]	$\frac{\exp\left(-\frac{(s/T)^2+1}{4\log(1/\varepsilon)}\right)}{2\pi(T-is)}$	$\mathcal{O}\left(T \log \frac{1}{\varepsilon}\right)$	$\tilde{\mathcal{O}}\left(u_r \alpha_A T \log \frac{1}{\varepsilon}\right)$
This work	$\frac{1}{\sqrt{4\pi T}} \exp\left(-\frac{s^2}{4T}\right)$	$\mathcal{O}\left(\sqrt{T \log \frac{1}{\varepsilon}}\right)$	$\tilde{\mathcal{O}}\left(u_r \sqrt{\alpha_A T \log \frac{1}{\varepsilon}}\right)$

#### 4.5 Extension beyond the factorized generator $A = L^\dagger L$

In this subsection we extend the framework to time-independent generators  $A \in \mathbb{C}^{N \times N}$  that are not necessarily of the form  $L^\dagger L$ . For clarity, we focus on the homogeneous system

$$\frac{d}{dt} \mathbf{u}(t) = -A \mathbf{u}(t), \quad \mathbf{u}(0) = \mathbf{u}_0, \quad (4.21)$$

since the inhomogeneous case can be handled analogously via Duhamel's principle. Throughout this subsection we omit auxiliary workspace qubits used by reversible arithmetic and Hamiltonian simulation, as they are uncomputed at the end. We use the Cartesian decomposition

$$A = H_1 + iH_2, \quad H_1 := \frac{A + A^\dagger}{2}, \quad H_2 := \frac{A - A^\dagger}{2i}, \quad (4.22)$$

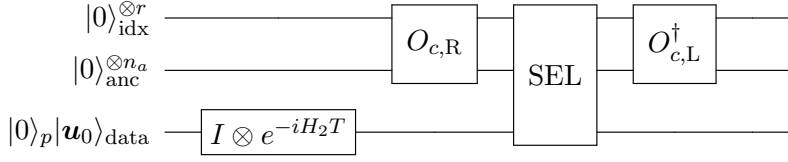


Fig. 3: Circuit for the normal case (4.26).

where  $H_1$  and  $H_2$  are Hermitian. Assuming  $H_1 \succeq 0$ , we may factor

$$H_1 = L^\dagger L \quad (4.23)$$

for some matrix  $L$ .

#### 4.5.1 Normal case $AA^\dagger = A^\dagger A$ .

If  $A$  is normal, then  $[H_1, H_2] = 0$  and the propagator factors as

$$\mathbf{u}(T) = e^{-AT} \mathbf{u}_0 = e^{-H_1 T} e^{-iH_2 T} \mathbf{u}_0 = e^{-L^\dagger L T} e^{-iH_2 T} \mathbf{u}_0. \quad (4.24)$$

We therefore first implement the unitary  $e^{-iH_2 T}$  by Hamiltonian simulation and then apply the dissipative factor  $e^{-L^\dagger L T}$  using the Kannai-transform LCU routine.

Let  $H$  be the Hermitian dilation associated with  $L$  as in (3.3) and define  $U(s) = e^{-iHs}$ . Set

$$U_{\kappa_T} := \int_{\mathbb{R}} \kappa_T(s) U(s) ds, \quad \kappa_T(s) = (4\pi T)^{-1/2} e^{-s^2/(4T)}.$$

After truncation and quadrature,  $U_{\kappa_T}$  is realized by an LCU unitary  $U_{\text{LCU},T}$ . Let  $n_a$  denote the number of ancilla qubits used by this LCU block.

Let the position qubit  $p$  encode the  $2 \times 2$  block structure and initialize  $|\psi_0\rangle := |0\rangle_p |\mathbf{u}_0\rangle_{\text{data}}$ . Then the Kannai representation reads

$$e^{-L^\dagger L T} |\mathbf{u}_0\rangle = (\langle 0|_p \otimes I) U_{\kappa_T} |\psi_0\rangle. \quad (4.25)$$

Combining (4.24) and (4.25), we obtain

$$|\mathbf{u}(T)\rangle \approx (\langle 0^{\otimes r}|_{\text{idx}} \langle 0^{\otimes n_a}|_{\text{anc}} \langle 0|_p \otimes I) U_{\text{LCU},T} |0^{\otimes r}\rangle_{\text{idx}} |0^{\otimes n_a}\rangle_{\text{anc}} |0\rangle_p (e^{-iH_2 T} |\mathbf{u}_0\rangle_{\text{data}}). \quad (4.26)$$

The overall circuit is shown in Fig. 3, and the query complexity is summarized in Corollary 4.1.

**Corollary 4.1.** *Let  $A \in \mathbb{C}^{N \times N}$  satisfy the decomposition (4.22) with  $H_1 \succeq 0$  and factorization  $H_1 = L^\dagger L$  as in (4.23), and assume  $[H_1, H_2] = 0$ . Assume (i) block-encoding access to  $L$  as in (4.2), and (ii) Hamiltonian-simulation access to  $H_2$ , e.g., via an  $(\alpha_{H_2}, a, 0)$  block-encoding oracle. Then the state  $|\mathbf{u}(T)\rangle \propto e^{-AT} |\mathbf{u}_0\rangle$  can be prepared using (4.26) up to accuracy  $\varepsilon$ , with total query complexity*

$$\tilde{\mathcal{O}}\left(u_r \left( \|L\| \sqrt{T \log \frac{u_r}{\varepsilon}} + \log \frac{u_r}{\varepsilon} + \alpha_{H_2} T \right)\right), \quad u_r := \frac{\|\mathbf{u}_0\|}{\|\mathbf{u}(T)\|},$$

up to polylogarithmic factors. Moreover, the number of calls to the state-preparation oracles is  $\mathcal{O}(u_r)$ .

### 4.5.2 Non-normal case $AA^\dagger \neq A^\dagger A$

We now consider the case  $AA^\dagger \neq A^\dagger A$ , so that  $[H_1, H_2] \neq 0$  and the exact factorization  $e^{-(H_1+iH_2)T} = e^{-H_1T}e^{-iH_2T}$  is unavailable. We adopt an operator-splitting approach. Let  $\tau := T/N_t$ . Using the second-order Strang splitting,

$$e^{-(H_1+iH_2)T} \approx \left( e^{-iH_2\tau/2} e^{-H_1\tau} e^{-iH_2\tau/2} \right)^{N_t}, \quad (4.27)$$

where the operator-norm error is controlled by commutators of  $H_1$  and  $H_2$  and scales as  $\mathcal{O}(\Lambda T\tau^2)$  under standard boundedness assumptions.

Let  $U_{\kappa_\tau} := \int_{\mathbb{R}} \kappa_\tau(s) U(s) ds$  be implemented by an LCU unitary  $U_{\text{LCU},\tau}$  with normalization  $\alpha_c(\tau) := \sum_{j=0}^{M-1} |c_j(\tau)| = \Theta(1)$ . Let  $n_a$  denote the number of ancilla qubits used by the LCU block. We combine it with the half-step unitary and set

$$U_\tau := (I \otimes e^{-iH_2\tau/2}) U_{\text{LCU},\tau} (I \otimes e^{-iH_2\tau/2}).$$

The success subspace is specified by the projector

$$\Pi := \left( |0^{\otimes r}\rangle_{\text{idx}} \langle 0^{\otimes r}| \right) \otimes \left( |0^{\otimes n_a}\rangle_{\text{anc}} \langle 0^{\otimes n_a}| \right) \otimes \left( |0\rangle_p \langle 0| \right) \otimes I_{\text{data}}, \quad (4.28)$$

which enforces the projection onto  $p = 0$ . For any  $|\psi\rangle \in \text{img}(\Pi)$ , the postselected branch satisfies

$$\Pi U_\tau |\psi\rangle \approx \frac{1}{\alpha_c(\tau)} W_\tau |\psi\rangle,$$

up to the step implementation error, where  $W_\tau$  denotes the induced Strang step on the physical state.

To avoid intermediate measurements, we apply robust oblivious amplitude amplification [18, Theorem 15] and choose an odd integer  $n$  such that  $\sin(\pi/(2n)) \approx 1/\alpha_c(\tau)$ . This yields

$$\tilde{U}_\tau = U_\tau \left( R_\Pi U_\tau^\dagger R_\Pi U_\tau \right)^{(n-1)/2}, \quad R_\Pi := I - 2\Pi, \quad n = \Theta(1),$$

which approximately maps  $\text{img}(\Pi)$  to itself and implements  $W_\tau$  on the success branch. Starting from  $|0^{\otimes r}\rangle_{\text{idx}} |0^{\otimes n_a}\rangle_{\text{anc}} |0\rangle_p |\mathbf{u}_0\rangle_{\text{data}}$ , we iterate coherently for  $N_t$  steps and measure the success flag once at the end:

$$|\mathbf{u}(T)\rangle \approx (\langle 0^{\otimes r}|_{\text{idx}} \langle 0^{\otimes n_a}|_{\text{anc}} \langle 0|_p \otimes I) (\tilde{U}_\tau)^{N_t} |0^{\otimes r}\rangle_{\text{idx}} |0^{\otimes n_a}\rangle_{\text{anc}} |0\rangle_p |\mathbf{u}_0\rangle_{\text{data}}. \quad (4.29)$$

**Corollary 4.2.** *Let  $A \in \mathbb{C}^{N \times N}$  admit the decomposition (4.22) with  $H_1 \succeq 0$  and factorization  $H_1 = L^\dagger L$  as in (4.23), and assume  $[H_1, H_2] \neq 0$ . Fix  $T > 0$  and a target accuracy  $\varepsilon \in (0, 1)$ . Consider the second-order Strang splitting (4.27) with step size  $\tau = T/N_t$ , and define*

$$\Lambda := \| [H_2, [H_2, H_1]] \| + \| [H_1, [H_1, H_2]] \|.$$

*Then the splitting error satisfies*

$$\left\| e^{-(H_1+iH_2)T} - \left( e^{-iH_2\tau/2} e^{-H_1\tau} e^{-iH_2\tau/2} \right)^{N_t} \right\| = \mathcal{O}(\Lambda T\tau^2)$$

in operator norm, and it suffices to choose

$$N_t = \Theta\left(\sqrt{\Lambda T^3/\varepsilon}\right).$$

Assume (i) block-encoding access to  $L$  as in (4.2), and (ii) Hamiltonian-simulation access to  $H_2$ , for instance via an  $(\alpha_{H_2}, a, 0)$  block-encoding oracle. Then the state  $|\mathbf{u}(T)\rangle \propto e^{-AT}|\mathbf{u}_0\rangle$  can be prepared using (4.29) up to accuracy  $\varepsilon$  with total query complexity

$$\tilde{\mathcal{O}}\left(u_r\left(\|L\|\left(\frac{\Lambda T^5}{\varepsilon}\right)^{1/4} + \sqrt{\frac{\Lambda T^3}{\varepsilon}} \log\frac{u_r}{\varepsilon} + \alpha_{H_2}T\right)\right),$$

up to polylogarithmic factors. Here  $u_r := \|\mathbf{u}_0\|/\|\mathbf{u}(T)\|$ , and the number of calls to the state-preparation oracles is  $\mathcal{O}(u_r)$ .

**Remark 4.2.** If  $[H_1, H_2] = 0$  and  $H_1 = L^\dagger L$ , then  $e^{-(H_1+iH_2)T} = e^{-H_1T}e^{-iH_2T}$ . With block-encoding access to  $L$ , the Kannai-transform LCU implements  $e^{-H_1T}$  and achieves the scaling in Corollary 4.1 up to polylogarithmic factors.

If  $[H_1, H_2] \neq 0$ , we combine the same Kannai-based step for  $e^{-H_1\tau}$  with Strang splitting and robust oblivious amplitude amplification. In stiff regimes  $\|H_1\| \gtrsim 1/\varepsilon$  and  $T = \mathcal{O}(1)$ , the resulting complexity can remain smaller than methods with linear dependence on  $\|H_1\|$  or  $\|A\|$ .

## 5 Complexity for representative PDEs

In this section, we instantiate the general complexity bound in Theorem 4.1 for representative partial differential equations. We focus on how boundary conditions and spatial discretization determine the operator norm  $\|L\|$ , and hence the overall query complexity of the proposed quantum algorithm.

### 5.1 The heat equation

We begin with the heat equation on a bounded domain  $\Omega \subset \mathbb{R}^d$ ,

$$\partial_t u = -\mathcal{A}u + f, \quad \mathcal{L} = -\nabla, \quad \mathcal{L}^\dagger = \operatorname{div}, \quad u(0, x) = u_0(x),$$

so that  $\mathcal{A} = \mathcal{L}^\top \mathcal{L} = -\operatorname{div} \nabla$ . Consider Dirichlet boundary data

$$u(t, x)|_{x \in \partial\Omega} = u_d(x), \quad t \geq 0.$$

In the first-order embedding  $\psi = [w \ v]^\top$ , the boundary condition is imposed on the auxiliary variable  $w$  by requiring

$$w(s, x)|_{x \in \partial\Omega} = u_d(x), \quad \text{for all } s.$$

Since the reconstruction uses the projection  $\Pi_1 \psi = w$ , the recovered solution  $u(t, \cdot)$  inherits the prescribed Dirichlet values.

We discretize the first-order system for  $\psi = [w \ v]^\top$  on a staggered grid such that the discrete gradient and divergence are represented by  $-L$  and  $L^\top$ , respectively.

In one dimension, let  $\Omega = (0, 1)$  and  $h = 1/N_x$ . Place  $w$  on primary nodes  $x_i = ih$  and  $v$  on midpoints  $x_{i+\frac{1}{2}} = (i + \frac{1}{2})h$ . Collect

$$\mathbf{w}_h(s) = (w_1(s), \dots, w_{N_x-1}(s))^\top \in \mathbb{R}^{N_x-1}, \quad \mathbf{v}_h(s) = (v_{1/2}(s), \dots, v_{N_x-1/2}(s))^\top \in \mathbb{R}^{N_x},$$

and enforce Dirichlet data by fixing  $w_0(s) = u_d(x_0)$  and  $w_{N_x}(s) = u_d(x_{N_x})$  for all  $s$ . Define  $L^{(1)} \in \mathbb{R}^{N_x \times (N_x-1)}$  by

$$(L^{(1)} \mathbf{w}_h)_{i+\frac{1}{2}} := -\frac{w_{i+1} - w_i}{h}, \quad i = 0, \dots, N_x - 1, \quad L^{(1)} = \frac{1}{h} \begin{bmatrix} -1 & & & & \\ 1 & -1 & & & \\ & \ddots & \ddots & & \\ & & 1 & -1 & \\ & & & & 1 \end{bmatrix}. \quad (5.1)$$

Then  $(\nabla w)_{i+\frac{1}{2}} \approx -(L^{(1)} \mathbf{w}_h)_{i+\frac{1}{2}}$  and  $(\operatorname{div} v)_i \approx ((L^{(1)})^\top \mathbf{v}_h)_i$ . We write  $L := L^{(1)}$  in one dimension.

In  $d$  dimensions on  $\Omega = (0, 1)^d$ , order interior nodal values of  $w$  into  $\mathbf{w}_h(s) \in \mathbb{R}^{M_w}$  with  $M_w = (N_x - 1)^d$ , and collect staggered face values of  $v$  into  $\mathbf{v}_h(s) \in \mathbb{R}^{M_v}$ . Lift  $L^{(1)}$  to each coordinate direction by

$$L^{(k)} = I_{N_x-1}^{\otimes(k-1)} \otimes L^{(1)} \otimes I_{N_x-1}^{\otimes(d-k)}, \quad k = 1, \dots, d, \quad (5.2)$$

and stack the directional operators as

$$L = \begin{bmatrix} (L^{(1)})^\dagger & (L^{(2)})^\dagger & \dots & (L^{(d)})^\dagger \end{bmatrix}^\dagger.$$

Then  $L : \mathbb{R}^{M_w} \rightarrow \mathbb{R}^{M_v}$  discretizes  $-\nabla$  on the staggered grid and  $L^\top$  discretizes  $\operatorname{div}$ . The semi-discrete first-order system is obtained from the continuum formulation by replacing  $(\mathcal{L}, \mathcal{L}^\top)$  with  $(L, L^\top)$ .

**Remark 5.1.** For homogeneous Neumann data  $\partial_n u = 0$  on  $\partial\Omega$ , it is natural to impose the boundary condition on the flux component. One convenient staggered placement samples  $v$  on primary nodes and  $w$  on staggered locations, so that the normal component of  $v$  can be fixed to zero on  $\partial\Omega$ . The resulting discrete gradient–divergence pair has the same structure as above, with the roles of  $w$  and  $v$  interchanged.

The following corollary specializes Theorem 4.1 to the heat equation under the staggered finite-difference discretization described above.

**Corollary 5.1.** *Consider  $\Omega = (0, 1)^d$  and the staggered finite-difference discretization above with mesh size  $h$  in each coordinate direction. Let  $L$  denote the resulting discrete gradient operator, and let  $H$  be the Hermitian dilation Hamiltonian constructed from  $L$  as in Section 4. Assume the hypotheses of Theorem 3.1 hold. Then the quantum algorithm in Theorem 4.1 prepares an  $\varepsilon$ -approximation of the normalized solution state  $|\mathbf{u}_h(T)\rangle$  with  $\Omega(1)$  success probability and a success flag, using*

$$\mathcal{O}\left(u_r \left(\frac{\sqrt{d}}{h} \sqrt{T \log \frac{u_r}{\varepsilon}} + \log \frac{u_r}{\varepsilon}\right)\right)$$

queries to the block-encoding oracle for  $H$ , where

$$u_r = \mathcal{O}\left(\frac{\|u_0\|_{L^2(\Omega)} + T\|f\|_{L^2(\Omega)}}{\|u(T)\|_{L^2(\Omega)}}\right).$$

Moreover, the number of calls to the state-preparation oracles  $O_\psi$  and  $O_b$  is  $\mathcal{O}(u_r)$ .

*Proof.* For the staggered finite-difference discretization on  $(0, 1)^d$ , the discrete gradient operator satisfies  $\|L\| = \Theta(\sqrt{d}/h)$ . Substituting this bound into Theorem 4.1 yields the stated query complexity. The bound on the number of calls to  $O_\psi$  and  $O_b$  follows from the same theorem.  $\square$

## 5.2 Viscous Hamilton–Jacobi equations via entropy penalisation

Hamilton–Jacobi equations are fundamental in mechanics and optimal control, and finite-time singularities motivate vanishing-viscosity regularisation and viscosity solutions, yielding (5.3). We then follow the entropy penalisation framework of [19, 25] to connect the regularised nonlinear dynamics to a linear parabolic surrogate suitable for quantum algorithms. Throughout this subsection, we restrict to the simplest setting where the viscosity coefficient is constant in space and time. Introducing the effective viscosity  $\bar{\nu} := 2a\nu$ , we consider on  $\mathbb{T}^d$  the viscous Hamilton–Jacobi equation

$$\partial_t S(t, x) + H(x, \nabla S(t, x)) = \bar{\nu} \Delta S(t, x), \quad S(0, x) = S_0(x), \quad (5.3)$$

where  $\nu > 0$  is the viscosity parameter and  $a > 0$  is the calibration constant induced by the entropy-penalisation kernel in [25], whose value depends on the Hamiltonian and the kernel choice, and it enters only through the effective viscosity  $\bar{\nu} = 2a\nu$  in (5.3).

The Hamiltonian is defined by a strictly convex kinetic energy  $K(v)$  and a potential  $V(x)$  via

$$H(x, p) = \sup_{v \in \mathbb{R}^d} (-p \cdot v - K(v) + V(x)) = V(x) + K^*(-p). \quad (5.4)$$

The continuous-time limit of the penalised scheme yields a constant-coefficient linear parabolic equation for an auxiliary variable  $u$  [25, Lemma 5],

$$\partial_t u(t, x) = \mu \cdot \nabla u(t, x) + \nabla \cdot (\Sigma \nabla u(t, x)), \quad u(0, x) = u_0(x), \quad (5.5)$$

where the drift  $\mu \in \mathbb{R}^d$  and the diffusion matrix  $\Sigma \in \mathbb{R}^{d \times d}$  are constants determined by  $K$  and  $\nu$ ,

$$v^* := \arg \min_{v \in \mathbb{R}^d} K(v), \quad \mu = v^*, \quad \Sigma = v^*(v^*)^\dagger + 2\nu(\nabla^2 K(v^*))^{-1}. \quad (5.6)$$

The viscosity solution is recovered from  $u$  through the Hopf–Cole transform [14, 24]

$$S_\nu(t, x) = -2\nu \log u(t, x), \quad (5.7)$$

up to an additive normalisation constant. In particular, when  $S_\nu$  satisfies a closed viscous Hamilton–Jacobi-type equation, the quadratic term induced by the diffusion in (5.5) involves the same matrix  $\Sigma$ , namely

$$\partial_t S_\nu(t, x) + \frac{1}{2\nu} \nabla S_\nu(t, x)^\dagger \Sigma \nabla S_\nu(t, x) - \mu \cdot \nabla S_\nu(t, x) = \nabla \cdot (\Sigma \nabla S_\nu(t, x)). \quad (5.8)$$

Since  $\mu$  is constant, we remove the drift by the translation

$$\tilde{u}(t, x) := u(t, x + \mu t), \quad (5.9)$$

so that  $\tilde{u}$  solves the constant-coefficient diffusion equation

$$\partial_t \tilde{u}(t, x) = \nabla \cdot (\Sigma \nabla \tilde{u}(t, x)) =: -\mathcal{A} \tilde{u}(t, x). \quad (5.10)$$

This subsection quantifies the quantum query complexity for the linear surrogate (5.10). A full end-to-end analysis for the original nonlinear viscosity solution and comparisons with classical methods are given in [25].

For the complexity estimate below we further specialise to the isotropic constant case  $\Sigma = \nu I_d$ , so that  $\mathcal{A} = -\nu \Delta$  in (5.10). Let  $N$  be the number of grid points per direction and set  $h := 1/N$ . On the periodic grid

$$\mathcal{G}_h := \{ \mathbf{x}_n = h \mathbf{n} : \mathbf{n} \in \{0, 1, \dots, N-1\}^d \},$$

we represent  $\tilde{u}(t, \cdot)$  by the value vector  $\tilde{\mathbf{u}}_h(t) \in \mathbb{C}^{N^d}$  defined through  $(\tilde{\mathbf{u}}_h(t))_{\mathbf{n}} := \tilde{u}(t, \mathbf{x}_n)$ . Let  $U_F$  be the unitary discrete Fourier transform and define the Fourier coefficient vector

$$\hat{\mathbf{u}}(t) := U_F \tilde{\mathbf{u}}_h(t), \quad \tilde{\mathbf{u}}_h(t) = U_F^\dagger \hat{\mathbf{u}}(t).$$

The Fourier basis is indexed by  $\mathbf{k} = (k_1, \dots, k_d) \in \mathcal{K}$  with

$$\mathcal{K} := \left\{ -\frac{N}{2}, -\frac{N}{2} + 1, \dots, \frac{N}{2} - 1 \right\}^d \subset \mathbb{Z}^d \quad (N \text{ even}), \quad \|\mathbf{k}\|^2 := \sum_{r=1}^d k_r^2.$$

The semi-discrete generator admits the diagonalisation

$$A = U_F^\dagger D U_F, \quad L_{\text{HJ}} := D^{1/2} U_F, \quad A = L_{\text{HJ}}^\dagger L_{\text{HJ}}, \quad (5.11)$$

where  $D$  is diagonal in the  $\mathbf{k}$ -basis with symbol  $D(\mathbf{k}) = \nu(2\pi)^2 \|\mathbf{k}\|^2$ . Consequently,

$$\|L_{\text{HJ}}\| = \|D^{1/2}\| = \max_{\mathbf{k}} \sqrt{D(\mathbf{k})} \leq \frac{\pi \sqrt{d \nu}}{h}. \quad (5.12)$$

Applying Theorem 4.1 to the homogeneous semi-discrete system  $d\tilde{\mathbf{u}}_h/dt = -A \tilde{\mathbf{u}}_h$  yields the following bound.

**Corollary 5.2.** *Let  $A$  and  $L_{\text{HJ}}$  be defined in (5.11). There exists a quantum algorithm that prepares an  $\varepsilon$ -approximation of the normalized state  $|\tilde{\mathbf{u}}_h(T)\rangle$  with  $\Omega(1)$  success probability and query complexity*

$$\tilde{\mathcal{O}}\left(u_r \left( \frac{\sqrt{d\nu}}{h} \sqrt{T \log\left(\frac{u_r}{\varepsilon}\right)} + \log\left(\frac{u_r}{\varepsilon}\right) \right)\right), \quad u_r := \frac{\|\tilde{\mathbf{u}}_h(0)\|}{\|\tilde{\mathbf{u}}_h(T)\|}.$$

Once  $|\tilde{\mathbf{u}}_h(T)\rangle$  is prepared, one may recover  $S_\nu(T, x)$  from (5.7) after estimating the required amplitudes of  $u(T, \cdot)$ .

### 5.3 Biharmonic diffusion equation

We next consider the biharmonic diffusion equation

$$\partial_t u = \Delta^2 u + f, \quad u(0, x) = u_0(x), \quad x \in \Omega \subset \mathbb{R}^d.$$

We impose boundary conditions so that  $-\Delta^2$  is self-adjoint and nonnegative on  $L^2(\Omega)$ , e.g., the simply supported plate conditions

$$u = 0, \quad \Delta u = 0 \quad \text{on } \partial\Omega.$$

Then  $\mathcal{A} := (-\Delta)^2 = \mathcal{L}^\top \mathcal{L}$  with  $\mathcal{L} := -\Delta$ . In the first-order embedding  $\psi = [w \ v]^\top$  in (2.6)–(2.7), we impose the homogeneous boundary conditions

$$w(t, s, \cdot) = 0, \quad v(t, s, \cdot) = 0 \quad \text{on } \partial\Omega.$$

We discretize  $-\Delta$  by standard second-order finite differences on a uniform grid with mesh size  $h = 1/N_x$ . In one dimension, collecting interior nodal values into  $\mathbf{w}_h(s), \mathbf{v}_h(s) \in \mathbb{R}^{N_x-1}$  and enforcing homogeneous Dirichlet data, we obtain

$$-(\Delta w)_i \approx (L^{(1)} \mathbf{w}_h)_i, \quad -(\Delta v)_i \approx ((L^{(1)})^\top \mathbf{v}_h)_i, \quad i = 1, \dots, N_x - 1,$$

with

$$L^{(1)} = \frac{1}{h^2} \begin{bmatrix} 2 & -1 & & & & \\ -1 & 2 & -1 & & & \\ & \ddots & \ddots & \ddots & & \\ & & -1 & 2 & -1 & \\ & & & -1 & 2 & \end{bmatrix}. \quad (5.13)$$

In  $d$  dimensions on  $\Omega = (0, 1)^d$ , letting  $M = (N_x - 1)^d$  and identifying  $\mathbf{w}_h(s), \mathbf{v}_h(s) \in \mathbb{R}^M$ , we define the discrete Laplacian by the Kronecker sum

$$L := \sum_{k=1}^d \left( I_{N_x-1}^{\otimes(k-1)} \otimes L^{(1)} \otimes I_{N_x-1}^{\otimes(d-k)} \right),$$

so that  $L$  is symmetric positive definite and approximates  $-\Delta$  with homogeneous Dirichlet data.

**Corollary 5.3.** *Consider the biharmonic diffusion equation on  $\Omega = (0, 1)^d$  with mesh size  $h = 1/N_x$  and the discretization above. Let  $L$  be the discrete Laplacian and let  $H$  be the Hermitian dilation Hamiltonian constructed from  $L$  as in Section 4. Assume the hypotheses of Theorem 3.1 hold. Then the quantum algorithm in Theorem 4.1 prepares an  $\varepsilon$ -approximation of the normalized discrete solution state  $|\mathbf{u}_h(T)\rangle$  with  $\Omega(1)$  success probability, using*

$$\tilde{\mathcal{O}}\left(u_r \left( \frac{d}{h^2} \sqrt{T \log \frac{u_r}{\varepsilon}} + \log \frac{u_r}{\varepsilon} \right) \right)$$

queries to the block-encoding oracle for  $H$ , where

$$u_r = \mathcal{O}\left(\frac{\|u_0\|_{L^2(\Omega)} + T\|f\|_{L^2(\Omega)}}{\|u(T)\|_{L^2(\Omega)}}\right).$$

Moreover, the number of calls to the state-preparation oracles for  $\psi_0$  and  $\mathbf{b}$  is  $\mathcal{O}(u_r)$ .

*Proof.* For this discretization,  $\|L\| = \mathcal{O}(d/h^2)$ . The claim follows by substituting this bound into Theorem 4.1.  $\square$

## 6 Long-time simulation for the dissipative dynamics and linear algebra problems

The query complexity bound in Theorem 4.1 depends explicitly on the final time parameter  $T$  through a polynomial-type dependence, up to polylogarithmic factors. In the long-time regime for strictly dissipative generators, however, the dependence on the physical final time can be removed.

Assume that  $\mathcal{A} = \mathcal{L}^\top \mathcal{L}$  is self-adjoint and has a spectral gap  $\sigma(\mathcal{A}) \subset [\lambda_0, \infty)$  for some  $\lambda_0 > 0$ . Then the semigroup decays exponentially,

$$\|e^{-\mathcal{A}T}\|_{L(L^2(\Omega), L^2(\Omega))} := \sup_{v \in L^2(\Omega)} \frac{\|e^{-\mathcal{A}T}v\|_{L^2(\Omega)}}{\|v\|_{L^2(\Omega)}} \leq e^{-\lambda_0 T},$$

and by Duhamel's principle

$$u(T) = e^{-\mathcal{A}T}u_0 + \int_0^T e^{-\mathcal{A}(T-s)}f \, ds = \mathcal{A}^{-1}f + e^{-\mathcal{A}T}(u_0 - \mathcal{A}^{-1}f).$$

Consequently,

$$\|u(T) - \mathcal{A}^{-1}f\|_{L^2(\Omega)} \leq e^{-\lambda_0 T} \|u_0 - \mathcal{A}^{-1}f\|_{L^2(\Omega)}.$$

Given any target accuracy  $\varepsilon > 0$ , it is sufficient to simulate the dynamics up to the truncated time

$$\tilde{T} := \frac{1}{\lambda_0} \log \frac{C}{\varepsilon},$$

for a problem-dependent constant  $C \geq \|u_0 - \mathcal{A}^{-1}f\|_{L^2(\Omega)}$ , in order to ensure  $\|u(T) - \mathcal{A}^{-1}f\|_{L^2(\Omega)} \leq \varepsilon$  for all  $T \geq \tilde{T}$ . In particular, the contribution of the initial datum is exponentially suppressed, and one may apply Theorem 4.1 with the time parameter set to  $\tilde{T}$ , so that the resulting query complexity depends on  $\tilde{T}$  rather than on the physical final time  $T$ .

Combining this observation with Theorem 4.1, we obtain the query complexity of our quantum algorithm in the long-time regime  $T \gg \lambda_0^{-1} \log(1/\varepsilon)$ .

**Corollary 6.1.** *Assume that  $\mathcal{A} = \mathcal{L}^\top \mathcal{L}$  is self-adjoint, and that the assumptions of Theorem 4.1 hold. Let  $\lambda_0 > 0$  denote a spectral gap of  $\mathcal{A}$ , namely  $\sigma(\mathcal{A}) \subset [\lambda_0, \infty)$ . Let  $\tilde{T} = \lambda_0^{-1} \log(C/\varepsilon)$  with  $C \geq \|\mathcal{A}^{-1}f\|_{L^2(\Omega)}$ , and consider the semi-discrete problem (3.2) on the time interval  $[0, \tilde{T}]$  with initial data set to zero. Then the quantum algorithm in Theorem 4.1, applied with  $T = \tilde{T}$  and  $u_0 = 0$ , prepares an  $\varepsilon$ -approximation of the normalized discrete steady state corresponding to  $u_\infty = \mathcal{A}^{-1}b$  with  $\Omega(1)$  success probability. More precisely, letting*

$$u_r := \frac{\frac{1}{\lambda_0} \log \varepsilon^{-1} \|f\|_{L^2(\Omega)}}{\|u(T)\|_{L^2(\Omega)}},$$

the total number of queries to the Hamiltonian oracle  $L$  is

$$\tilde{\mathcal{O}}\left(\frac{\|f\|_{L^2(\Omega)}}{\lambda_0^{\frac{3}{2}} \|u(T)\|_{L^2(\Omega)}} (\log \frac{1}{\varepsilon})^2\right),$$

and the number of calls to the state-preparation oracle for  $\mathbf{b}$  is  $\mathcal{O}(u_r)$ .

**Remark 6.1.** Under the same dissipativity and gap assumptions, the LCHS-based long-time algorithm in [53] yields a query complexity independent of the physical final time  $T$ , with  $\tilde{\mathcal{O}}(\log^3(1/\varepsilon))$  dependence on the target accuracy. In contrast, Corollary 6.1 yields a  $T$ -independent complexity with polylogarithmic dependence

$$\tilde{\mathcal{O}}(\log^2(1/\varepsilon)),$$

thus improving the  $\varepsilon$ -dependence while working under the same dissipativity and gap assumptions on  $\mathcal{A}$ .

We now interpret the above long-time reduction as a linear systems solver for Hermitian positive definite problems  $A\mathbf{x} = \mathbf{b}$  with  $A = L^\top L$ . As is standard, we first rescale so that  $\|A\| = \mathcal{O}(1)$ : choose  $\alpha \geq \|A\|$  and consider

$$\frac{1}{\alpha} A \mathbf{x} = \frac{1}{\alpha} \mathbf{b}. \quad (6.1)$$

This does not change the solution, and it ensures  $\|A/\alpha\| \leq 1$  and  $\|L/\sqrt{\alpha}\| = \mathcal{O}(1)$ . Let

$$\lambda_{\min} := \lambda_{\min}(A), \quad \kappa := \frac{\lambda_{\max}(A)}{\lambda_{\min}(A)}$$

be the smallest eigenvalue and the condition number of the original matrix  $A$ . After normalization,  $\lambda_{\max}(A/\alpha) = \Theta(1)$  and hence  $\lambda_{\min}(A/\alpha) = \Theta(1/\kappa)$ , so the gap parameter in the long-time analysis satisfies  $\lambda_0 = \Theta(1/\kappa)$ .

Combining this normalization with Corollary 6.1 yields the following corollary; the proof follows by substituting  $\tilde{T} = \Theta(\kappa \log(1/\varepsilon))$  and the corresponding bound on  $u_r$  into Theorem 4.1.

**Corollary 6.2.** *Let  $A \in \mathbb{C}^{N \times N}$  be Hermitian positive definite and admit a factorization  $A = L^\dagger L$ . Assume the hypotheses of Theorem 4.1 hold. Then, for any  $0 < \varepsilon < 1$ , there exists a quantum algorithm that, given a block-encoding of  $L$  and a state-preparation oracle for  $\mathbf{b}$ , outputs with success probability  $\Omega(1)$  a normalized state  $|\mathbf{x}^{\text{out}}\rangle$  such that*

$$\| |\mathbf{x}^{\text{out}}\rangle - |\mathbf{x}\rangle \| \leq \varepsilon,$$

where  $\mathbf{x}$  is the solution to (6.1). The total number of queries to the block-encoding oracle for  $A$  constructed from  $L$  as in Section 4 is

$$\tilde{\mathcal{O}}\left(\kappa^{3/2} \left(\log \frac{1}{\varepsilon}\right)^2\right),$$

and the number of calls to the state-preparation oracle for  $\mathbf{b}$  is

$$\mathcal{O}\left(\kappa \log \frac{1}{\varepsilon}\right).$$

It is instructive to compare our complexity bounds with existing quantum linear systems algorithms. The original HHL algorithm [21] has query complexity  $\tilde{\mathcal{O}}(\kappa^2 \varepsilon^{-1})$ . Subsequent improvements based on the linear combination of unitaries (LCU) [12], quantum singular value transformation (QSVT) [18], and quantum signal processing (QSP) [40] reduce the dependence on  $\varepsilon$  to  $\tilde{\mathcal{O}}(\kappa^2 \text{polylog}(\kappa/\varepsilon))$ , but still exhibit quadratic scaling in  $\kappa$ . Schrödingerization-based linear system solvers further achieve query complexity of the form  $\tilde{\mathcal{O}}(\kappa^2 \log^3(1/\varepsilon))$ , again with a  $\kappa^2$  dependence on the condition number.

In contrast, Corollary 6.2 improves both the condition number dependence and the  $\varepsilon$ -dependence in this setting. While the  $\kappa^{3/2}$  scaling is slightly worse than the optimal  $\tilde{\mathcal{O}}(\kappa)$  achievable via variable-time amplitude amplification [12, 50], the resulting algorithm is simpler and already asymptotically better than HHL-type and Schrödingerization-based methods without preconditioning.

## 7 Other transmutation methods for quantum algorithms

We collect further examples where a non-unitary evolution can be represented as a superposition of reversible dynamics, consistent with the transmutation viewpoint.

Let  $\mathcal{A}$  be a linear operator and consider two evolution families  $w(s, \mathcal{A})$  and  $u(t, \mathcal{A})$ . Following [22], a transmutation from the  $s$ -dynamics to the  $t$ -dynamics is an identity of the form

$$u(t, \mathcal{A}) = \int_{\Gamma} K(t, s) w(s, \mathcal{A}) \, ds, \quad (7.1)$$

where the kernel  $K(t, s)$  is independent of the particular realization of  $\mathcal{A}$ . In the examples below,  $w(s, \mathcal{A})$  is unitary, or can be obtained from a unitary dynamics. The formula (7.1) then yields a continuous linear combination of unitary evolutions applied to the initial data.

### 7.1 Spherical means and the Euler–Poisson–Darboux equation

A classical example is the Euler–Poisson–Darboux equation [15]

$$u_{tt} + \frac{d-1}{t} u_t = \Delta_x u, \quad u(0, x) = u_0(x), \quad u_t(0, x) = 0.$$

If  $w$  solves the  $d$ -dimensional wave equation

$$w_{tt} = \Delta_x w, \quad w(0, x) = u_0(x), \quad w_t(0, x) = 0,$$

then the transmutation formula reads

$$u(t, x) = c_d \int_{-1}^1 w(\lambda t, x) (1 - \lambda^2)^{\frac{d-3}{2}} \, d\lambda, \quad (7.2)$$

which is a special case of the Delsarte–Lions transmutation [37, 38].

Introduce the first-order wave formulation similar to (2.6)–(2.8), one has

$$w(\cdot, s) = \Pi_1 \mathcal{U}(s) \psi_0, \quad \psi_0 = [u_0 \ 0]^\top,$$

where  $\mathcal{U}(s) = e^{s\tilde{\mathcal{L}}}$  with  $\tilde{\mathcal{L}} = -|0\rangle\langle 1| \otimes \mathcal{L}^\dagger + |1\rangle\langle 0| \otimes \mathcal{L}$ . Then (7.2) becomes

$$u(t, \cdot) = \frac{c_d}{t} \Pi_1 \int_{-t}^t \left(1 - \frac{s^2}{t^2}\right)^{\frac{d-3}{2}} \mathcal{U}(s) \psi_0 \, ds.$$

Approximating the integral by a quadrature with weights  $\{c_j\}_{j=1}^M$  and nodes  $\{s_j\}_{j=1}^M \subset [-t, t]$  yields an LCU form  $\sum_{j=1}^M c_j \mathcal{U}(s_j) \psi_0$  with coefficient  $\ell_1$ -norm  $\alpha_c = \sum_j |c_j| \approx \int_{-t}^t |K(t, s)| \, ds$ . Then, we have

$$\int_{-t}^t |K(t, s)| \, ds = \frac{c_d}{t} \int_{-t}^t \left(1 - \frac{s^2}{t^2}\right)^{\frac{d-3}{2}} \, ds = \mathcal{O}(c_d), \quad \text{hence} \quad \alpha_c = \mathcal{O}(c_d).$$

Therefore, for any target precision  $\varepsilon \in (0, 1)$ , there exists a quantum algorithm that prepares an  $\varepsilon$ -approximation of the normalized state proportional to  $u(T)$  with  $\Omega(1)$  success probability and a success flag, using

$$\tilde{\mathcal{O}}\left(\frac{c_d \|u_0\|_{L^2(\Omega)}}{\|u(T)\|_{L^2(\Omega)}} \|H\|T\right)$$

queries to a block-encoding of the Hermitian dilation Hamiltonian  $H$  associated with  $\tilde{\mathcal{L}}$ .

**Remark 7.1.** This transmutation perspective has two immediate advantages for quantum algorithms. First, it represents the non-unitary dynamics associated with the second-order-in-time equation as a continuous superposition of unitary wave propagators. Second, it removes the explicit time dependence in the coefficient  $(d-1)/t$  by transferring it to the integration kernel, while the underlying generator  $\tilde{\mathcal{L}}$  is time independent.

## 7.2 Transport–heat averaging

Following [43], consider the transport equation on  $\mathbb{R}^d$ ,

$$y_t + \alpha \cdot \nabla_x y = 0, \quad y(0, x; \alpha) = y_0(x),$$

where  $\alpha$  is a standard Gaussian random vector with density  $K(\alpha) = (2\pi)^{-d/2} e^{-|\alpha|^2/2}$ . The solution is  $y(t, x; \alpha) = y_0(x - t\alpha)$  and its average is

$$\tilde{y}(t, x) = \int_{\mathbb{R}^d} K(\alpha) y_0(x - t\alpha) d\alpha.$$

One checks that  $\tilde{y}$  satisfies

$$\tilde{y}_t = t^{-1} \Delta_x \tilde{y}, \quad \tilde{y}(0, \cdot) = y_0.$$

Defining  $u(t, x) := \tilde{y}(\sqrt{2t}, x)$  yields the heat equation

$$u_t - \Delta_x u = 0, \quad u(0, \cdot) = y_0.$$

In operator form, set  $\mathcal{T}(\alpha) := -\alpha \cdot \nabla_x$ . Then

$$u(t, \cdot) = \int_{\mathbb{R}^d} K(\alpha) e^{\sqrt{2t}\mathcal{T}(\alpha)} y_0 d\alpha, \quad (7.3)$$

and  $e^{s\mathcal{T}(\alpha)}$  is unitary on  $L^2(\mathbb{R}^d)$ .

For the periodic setting discretized by a Fourier spectral method, the discrete generator is skew-Hermitian and can be written as  $\mathcal{T}_h(\alpha) = -iH(\alpha)$  with  $H(\alpha)$  Hermitian. Truncating the Gaussian measure to  $|\alpha| \leq R_\alpha$  with  $R_\alpha = \mathcal{O}(\sqrt{\log(1/\varepsilon)})$  yields  $\|H(\alpha)\| = \mathcal{O}(R_\alpha \|H_0\|)$  for a fixed Hermitian matrix  $H_0$  determined by the spatial grid. The resulting quantum algorithm has query complexity

$$\tilde{\mathcal{O}}\left(\frac{\|u_0\|_{L^2(\Omega)}}{\|u(T)\|_{L^2(\Omega)}} \|H_0\| \sqrt{T \log \frac{1}{\varepsilon}}\right),$$

with polylogarithmic factors suppressed.

**Remark 7.2.** For the periodic heat equation, the transport–heat averaging representation (7.3) yields a quantum algorithm whose matrix-query complexity matches that of the Kannai-transform-based construction at the level of leading-order scaling in  $T$  and  $\varepsilon$ . However, this approach relies on the discrete transport generator  $\mathcal{T}_h(\alpha)$  being anti-Hermitian so that  $\exp(s\mathcal{T}_h(\alpha))$  is unitary. This is naturally satisfied by Fourier spectral discretizations under periodic boundary conditions, but it is incompatible with standard upwind schemes for first-order transport, which are dissipative and therefore do not yield an anti-Hermitian discrete operator. Moreover, extending the transport–averaging construction beyond periodic settings is nontrivial, since other boundary conditions and general domains do not preserve the simple translation structure underlying (7.3).

## 8 Numerical tests

In this section we present numerical experiments to validate (i) the correctness of the Kannai transform used to recover the heat solution from a wave equation and (ii) the correctness of the unitary embedding obtained via the first-order factorization. We consider the one-dimensional heat equation on  $\Omega = [0, 1]$ ,

$$\partial_t u(t, x) = \partial_{xx} u(t, x), \quad u(0, x) = u_0(x), \quad (8.1)$$

with two different boundary conditions. In both cases we compute the solution at  $T = 1$  and compare the Kannai-based solution with a classical finite-difference (FD) time-marching solution.

All results below are obtained via classical simulation and serve to validate (i) and (ii), rather than to demonstrate quantum speedup. We evaluate the truncated Kannai Gaussian integral on  $[-R, R]$  with  $R = 10$  using the trapezoidal rule with  $M = 800$  panels, and implement the unitary propagator  $e^{-iHs}$  in MATLAB via `expm` (i.e., `expm(-1i*H*s)`).

**Case 1: inhomogeneous Dirichlet boundary condition.** We impose

$$u(t, 0) = 1, \quad u(t, 1) = 1, \quad u_0(x) = \cos(2\pi x). \quad (8.2)$$

After spatial discretization with mesh size  $h = 1/N_x$  and  $N_x = 50$ , we introduce the first-order system  $\psi = [w; v]^\top$  as in Section 3.1 and obtain the inhomogeneous ODE

$$\frac{d}{ds} \psi_h(s) = \tilde{L} \psi_h(s) + \mathbf{f}_{\text{bd}}, \quad \tilde{L} = |0\rangle\langle 1| \otimes L^\dagger - |1\rangle\langle 0| \otimes L, \quad \mathbf{f}_{\text{bd}} = \frac{1}{h}(-\mathbf{e}_{N_x} + \mathbf{e}_{2N_x-1}), \quad (8.3)$$

where  $L$  is the staggered first-order difference operator in (5.1) and  $\mathbf{e}_j$  denotes the  $j$ -th standard basis vector.

Define  $U(s) = \exp(\tilde{L}s)$ . Following (3.4)–(3.12), we recover the heat solution by the Kannai transform

$$\mathbf{u}_f^{\text{disc}}(T) \approx \mathbf{u}_f^h(T) = \sum_{m=0}^M \omega_m \left( \kappa_T(s_m) U(s_m) \psi_0 + \Lambda_T(s_m) U(s_m) \mathbf{f}_{\text{bd}} \right), \quad (8.4)$$

where  $\{s_m\}_{m=0}^M$  are uniform nodes on  $[-R, R]$  given by  $s_m = -R + m\Delta s$  with  $\Delta s = 2R/M$ , and

$\{\omega_m\}_{m=0}^M$  are trapezoidal weights  $\omega_0 = \omega_M = \Delta s/2$  and  $\omega_m = \Delta s$  for  $1 \leq m \leq M-1$ . Here

$$\kappa_T(s) = \frac{1}{\sqrt{4\pi T}} e^{-s^2/(4T)}, \quad \Lambda_T(\sigma) = \begin{cases} \int_{\sigma}^{\infty} \kappa_T(s) ds = \frac{1}{2} \operatorname{erfc}\left(\frac{\sigma}{2\sqrt{T}}\right), & \sigma \geq 0, \\ - \int_{-\infty}^{\sigma} \kappa_T(s) ds = -\frac{1}{2} \operatorname{erfc}\left(\frac{-\sigma}{2\sqrt{T}}\right), & \sigma < 0. \end{cases}$$

We take the first  $N_x - 1$  components of  $\mathbf{u}_f^h(T)$  as the approximation of  $u(T, \cdot)$  on the interior grid. The numerical result is shown in the left panel of Fig. 4.

**Case 2: homogeneous Neumann boundary condition.** We impose

$$\partial_x u(t, 0) = \partial_x u(t, 1) = 0, \quad u_0(x) = \cos(\pi x). \quad (8.5)$$

Following Remark 5.1, we place  $w$  at cell centers and  $v$  at grid points, leading to the homogeneous semi-discrete system

$$\frac{d}{ds} \psi_h(s) = \tilde{L} \psi_h(s), \quad \tilde{L} = \begin{pmatrix} O & L^\dagger \\ -L & O \end{pmatrix}, \quad L^\dagger = \frac{1}{h} \begin{pmatrix} 1 & 0 & \cdots & 0 \\ -1 & 1 & \cdots & 0 \\ \vdots & \ddots & \ddots & \vdots \\ 0 & \cdots & -1 & 1 \\ 0 & \cdots & 0 & -1 \end{pmatrix}. \quad (8.6)$$

In this setting the evolution is unitary, and we compute  $\mathbf{u}_f^{\text{disc}}$  by

$$\mathbf{u}_f^{\text{disc}} = \int_{\mathbb{R}} \kappa_T(s) U(s) ds \psi_0 \approx \sum_{m=0}^M \omega_m \kappa_T(s_m) U(s_m) \psi_0 := \mathbf{u}_f^h(T).$$

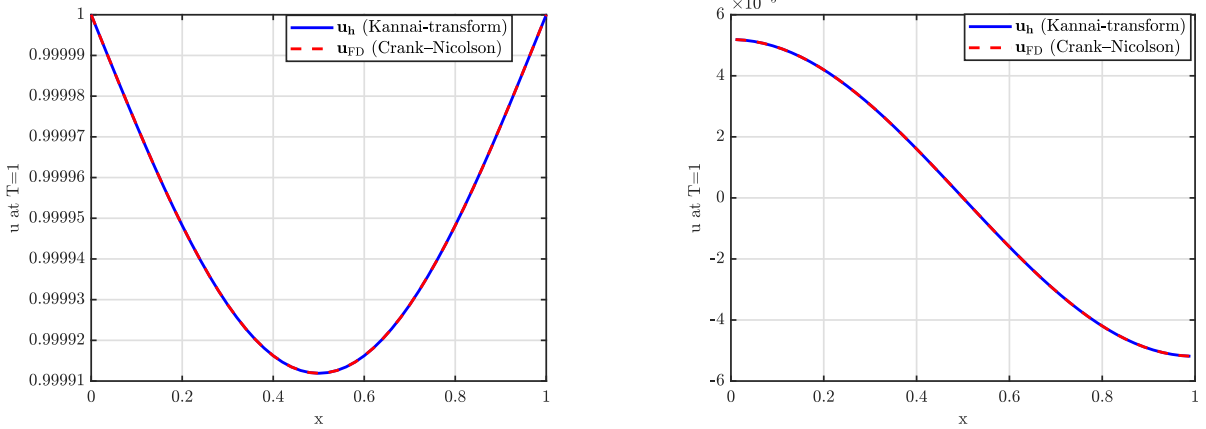
The right panel of Fig. 4 shows that the Kannai-based solution matches the classical FD solution very well.

In both boundary-condition settings, the numerical solutions obtained from the Kannai transform agree with the reference finite-difference solutions, which supports the correctness of (i) recovering the heat dynamics via the Kannai integral representation and (ii) the unitary embedding produced by the first-order factorization.

## 9 Conclusion

We introduced a Transmutation-based framework for quantum algorithms targeting dissipative evolution problems that arise from parabolic partial differential equations. After spatial discretization, these problems are governed by matrices with a special factorized structure given by the product of a matrix and its transpose. Building on the classical Kannai transform, which represents diffusion as a Gaussian-weighted average of wave-type dynamics, we reformulated the problem in a way that is directly compatible with standard tools from quantum Hamiltonian simulation.

On the classical side, we designed a fully discrete scheme based on spatial discretization and Gaussian quadrature in the auxiliary variable, together with explicit error estimates. On the quantum side, these estimates yield transparent bounds on the number of queries to the block-encoded wave Hamiltonian and to the state-preparation oracles. The resulting query complexity



(a) Case 1: Dirichlet  $u(t, 0) = u(t, 1) = 1$ .

(b) Case 2: Neumann  $\partial_x u|_{\partial\Omega} = 0$ .

Fig. 4: Comparison between the Kannai-based numerical solution and the classical finite-difference solution at  $T = 1$ .

grows with a *square-root* dependence on the evolution time, the size of the generator and only mild logarithmic dependence on the target accuracy. To the best of our knowledge, this places our method among the most efficient currently available quantum algorithms for non-unitary dynamics with such factorized generators.

We illustrated the approach on heat, viscous Hamilton-Jacobi and biharmonic diffusion, including several standard non-periodic boundary conditions, and explained how long-time evolution within this framework can be used to solve linear systems. Future work includes combining the transmutation-based method with quantum preconditioning, treating time-dependent and non-self-adjoint operators, and exploring connections with control and inverse problems.

## A Additional Technical Lemmas

We define

$$I_1 = \left( \int_{\mathbb{R}} \kappa_T(s) U(s) ds \right) \psi_0, \quad I_2 = \left( \int_{\mathbb{R}} \Lambda_T(\sigma) U(\sigma) d\sigma \right) \mathbf{b}.$$

**Lemma A.1.** Define the symmetric truncations on  $[-R, R]$

$$I_{1,\text{trunc}}^{(R)} = \left( \int_{-R}^R \kappa_T(s) U(s) ds \right) \psi_0, \quad I_{2,\text{trunc}}^{(R)} = \left( \int_{-R}^R \Lambda_T(\sigma) U(\sigma) d\sigma \right) \mathbf{b},$$

where  $\kappa_T(s)$  in (3.6) and  $\Lambda_T$  is defined in (3.8) Then the truncation errors satisfy

$$\|I_1 - I_{1,\text{trunc}}^{(R)}\| \leq \frac{2\sqrt{T}}{\sqrt{\pi} R} e^{-R^2/(4T)} \|\psi_0\|, \quad \text{and} \quad \|I_2 - I_{2,\text{trunc}}^{(R)}\| \leq \frac{4T\sqrt{T}}{R\sqrt{\pi}} e^{-R^2/(4T)} \|\mathbf{b}\|,$$

where  $I_1$  and  $I_2$  are defined in (3.5).

*Proof.* Since  $U(\cdot)$  is unitary,  $\|U(s)x\| = \|x\|$  for all  $s$ . For  $I_1$ , one has

$$\|I_1 - I_{1,\text{trunc}}^{(R)}\| \leq \int_{|s|>R} \kappa_T(s) ds \|\psi_0\| = \text{erfc}\left(\frac{R}{2\sqrt{T}}\right) \|\psi_0\|.$$

The stated exponential bound follows from  $\text{erfc}(z) \leq \frac{1}{\sqrt{\pi}z} e^{-z^2}$ .

For  $I_2$ , by oddness of  $\Lambda_T$  we have that  $|\Lambda_T|$  is even, and for  $\sigma \geq 0$ ,

$$0 \leq \Lambda_T(\sigma) = \frac{1}{\sqrt{4\pi T}} \int_{\sigma}^{\infty} e^{-s^2/(4T)} (s - \sigma) \, ds \leq \frac{1}{\sqrt{4\pi T}} \int_{\sigma}^{\infty} e^{-s^2/(4T)} s \, ds = \sqrt{\frac{T}{\pi}} e^{-\sigma^2/(4T)}.$$

Therefore, it yields

$$\|I_2 - I_{2,\text{trunc}}^{(R)}\| \leq \int_{|\sigma|>R} |\Lambda_T(\sigma)| \, d\sigma \, \|\mathbf{b}\| \leq 2\sqrt{\frac{T}{\pi}} \int_R^{\infty} e^{-\sigma^2/(4T)} \, d\sigma \, \|\mathbf{b}\|.$$

Using  $\int_R^{\infty} e^{-\sigma^2/(4T)} \, d\sigma = \sqrt{4\pi T} \Phi_T(R)$  and  $\Phi_T(R) = \frac{1}{2} \text{erfc}\left(\frac{R}{2\sqrt{T}}\right) \leq \frac{\sqrt{T}}{\sqrt{\pi}R} e^{-R^2/(4T)}$  gives the claimed bound.  $\square$

**Lemma A.2.** *Let  $\kappa_T$  and let  $\Lambda_T$  be defined in (3.6) and (3.8), respectively. Define the composite  $Q$ -point Gauss–Legendre approximations on  $[-R, R]$  with panel size  $h_1$ :*

$$I_{1,h} = \sum_{m=-R/h_1}^{R/h_1-1} \sum_{q=1}^Q w_{q,m} \kappa_T(s_{q,m}) U(s_{q,m}) \psi_0, \quad I_{2,h} = \sum_{m=-R/h_1}^{R/h_1-1} \sum_{q=1}^Q w_{q,m} \Lambda_T(s_{q,m}) U(s_{q,m}) \mathbf{b},$$

where  $s_{q,m}$  and  $w_{q,m}$  are given in (3.9). Then the quadrature errors satisfy

$$\|I_{1,h} - I_{1,\text{trunc}}^{(R)}\| \leq 2^{-2Q+1} R h_1^{2Q} \frac{1}{\sqrt{T}} \left( \|H\| + \frac{1}{\sqrt{2T}} \right)^{2Q} \|\psi_0\|, \quad (\text{A.1})$$

$$\|I_{2,h} - I_{2,\text{trunc}}^{(R)}\| \leq 2^{-2Q+1} R h_1^{2Q} \sqrt{T} \left( \|H\| + \frac{1}{\sqrt{2T}} \right)^{2Q} \|\mathbf{b}\|. \quad (\text{A.2})$$

*Proof.* We prove (A.1); the estimate (A.2) follows similarly. On each panel  $I_m = [mh_1, (m+1)h_1]$ , the  $Q$ -point Gauss–Legendre rule satisfies the classical bound

$$\left\| \int_{I_m} f(s) \, ds - Q_Q^{\text{GL}}(f) \right\| \leq C_Q^{\text{GL}} h_1^{2Q+1} \max_{s \in I_m} \|f^{(2Q)}(s)\|, \quad C_Q^{\text{GL}} = \frac{(Q!)^4}{(2Q+1)[(2Q)!]^3}.$$

Summing over all panels of  $[-R, R]$  gives

$$\|I_{1,h} - I_{1,\text{trunc}}^{(R)}\| \leq 2R C_Q^{\text{GL}} h_1^{2Q} \sup_{s \in [-R,R]} \|(\kappa_T U)^{(2Q)}(s)\| \|\psi_0\|. \quad (\text{A.3})$$

We next bound  $\sup_s \|(\kappa_T U)^{(2Q)}(s)\|$ . For  $k \geq 0$ ,

$$\kappa_T^{(k)}(s) = \frac{(-1)^k}{\sqrt{4\pi T}} \left( \frac{1}{2\sqrt{T}} \right)^k H_k \left( \frac{s}{2\sqrt{T}} \right) e^{-s^2/(4T)},$$

and using the standard estimate  $|H_k(x)| \leq 2^{k/2} \sqrt{(2k)!} e^{x^2/2}$  yields

$$\sup_{s \in \mathbb{R}} |\kappa_T^{(k)}(s)| \leq A_k T^{-(k+1)/2}, \quad A_k := \frac{2^{-k/2} \sqrt{(2k)!}}{\sqrt{\pi}}. \quad (\text{A.4})$$

Moreover,  $U^{(j)}(s) = (-iH)^j U(s)$  implies  $\|U^{(j)}(s)\| \leq \|H\|^j$ . By Leibniz' rule, it yields

$$\sup_{s \in [-R,R]} \|(\kappa_T U)^{(2Q)}(s)\| \leq \sum_{k=0}^{2Q} \binom{2Q}{k} \sup_s |\kappa_T^{(k)}(s)| \sup_s \|U^{(2Q-k)}(s)\| \leq \frac{C_Q^{\kappa}}{\sqrt{T}} \left( \|H\| + \frac{1}{\sqrt{2T}} \right)^{2Q},$$

for a constant  $C_Q^\kappa = \sqrt{(4Q)!}$  depending only on  $Q$ . Substituting this bound into (A.3) and using  $2R C_Q^{\text{GL}} C_Q^\kappa \leq 2^{-2Q+1} R$  gives (A.1).

For  $I_2$ , one applies the same argument to  $f(s) = \Lambda_T(s)U(s)$ . Note that  $\sup_\sigma |\Lambda_T(\sigma)| = \Lambda_T(0) = \sqrt{T/\pi}$ , and for  $\sigma \neq 0$ ,  $\Lambda'_T(\sigma) = -\Phi_T(\sigma)$  for  $\sigma > 0$  and  $\Lambda'_T(\sigma) = -(1 - \Phi_T(\sigma)) = -\Phi_T(-\sigma)$  for  $\sigma < 0$ , with  $\Phi'_T(\sigma) = -\kappa_T(\sigma)$ . Thus,  $\Lambda_T^{(k)}$  can be bounded in terms of derivatives of  $\kappa_T$ , yielding an overall prefactor of order  $\sqrt{T}$  and leading to (A.2).  $\square$

**Lemma A.3.** *Assume the offline kernels  $\kappa_T^a$  and  $\Lambda_T^a$  satisfy (3.10) and (3.11), respectively. The discrete sums satisfy*

$$\sum_{m,q} |c_{q,m}| \leq (1 + \delta_{\text{off}}) + 2^{-2Q+1} \frac{R}{\sqrt{T}} \left( \frac{h_1}{\sqrt{T}} \right)^{2Q}, \quad (\text{A.5})$$

$$\sum_{m,q} |d_{q,m}| \leq (1 + \delta_{\text{off}}) T + 2^{-2Q+1} R \sqrt{T} \left( \frac{h_1}{\sqrt{T}} \right)^{2Q}. \quad (\text{A.6})$$

*Proof.* We bound the two sums separately. Since  $\kappa_T \geq 0$ , (3.10) implies  $|\kappa_T^a(s)| \leq (1 + \delta_{\text{off}})\kappa_T(s)$  for all  $s$ , hence

$$\sum_{m,q} |c_{q,m}| \leq (1 + \delta_{\text{off}}) \sum_{m,q} w_{q,m} \kappa_T(s_{q,m}).$$

The right-hand side is the composite Gauss–Legendre approximation of  $\int_{-R}^R \kappa_T(s) ds$ , so

$$\sum_{m,q} w_{q,m} \kappa_T(s_{q,m}) \leq \int_{-R}^R \kappa_T(s) ds + \left| \int_{-R}^R \kappa_T(s) ds - \sum_{m,q} w_{q,m} \kappa_T(s_{q,m}) \right|.$$

Using  $\int_{-\infty}^{\infty} \kappa_T(s) ds = 1$  gives  $\int_{-R}^R \kappa_T(s) ds \leq 1$ . Moreover, the standard  $Q$ -point Gauss–Legendre error bound on each panel and summation over  $[-R, R]$  yield

$$\left| \int_{-R}^R \kappa_T(s) ds - \sum_{m,q} w_{q,m} \kappa_T(s_{q,m}) \right| \leq 2R C_Q^{\text{GL}} h_1^{2Q} \sup_{s \in [-R, R]} |\kappa_T^{(2Q)}(s)|.$$

its derivatives, from (A.4), gives (A.5).

For  $d_{q,m}$ , (3.11) yields  $|\Lambda_T^a(s)| \leq (1 + \delta_{\text{off}})|\Lambda_T(s)|$ . Hence

$$\sum_{m,q} |d_{q,m}| \leq (1 + \delta_{\text{off}}) \sum_{m,q} w_{q,m} |\Lambda_T(s_{q,m})|.$$

As above, this is a composite Gauss–Legendre approximation of  $\int_{-R}^R |\Lambda_T(\sigma)| d\sigma$ , so it is bounded by that integral plus the quadrature error on  $[-R, R]$ . By Fubini’s Theorem and symmetry,

$$\int_{-\infty}^{\infty} |\Lambda_T(\sigma)| d\sigma = 2 \int_0^{\infty} \Lambda_T(\sigma) d\sigma = \frac{1}{\sqrt{4\pi T}} \int_0^{\infty} \frac{s^2}{2} e^{-s^2/(4T)} ds = T,$$

hence  $\int_{-R}^R |\Lambda_T(\sigma)| d\sigma \leq T$ . Finally,  $|\Lambda_T|$  is smooth on  $\mathbb{R} \setminus \{0\}$  and satisfies  $\sup_\sigma |\Lambda_T(\sigma)| = \Lambda_T(0) = \sqrt{T/\pi}$ , and the same panelwise Gauss–Legendre estimate yields a quadrature remainder bounded by  $2^{-2Q+1} R \sqrt{T} \left( \frac{h_1}{\sqrt{T}} \right)^{2Q}$  after combining derivative bounds. This proves (A.6).  $\square$

**Lemma A.4.** Assume that the offline kernels  $\kappa_T^a$  and  $\Lambda_T^a$  satisfy (3.10) and (3.11), respectively. Define the discrete quadrature approximations on  $[-R, R]$

$$I_{1,h}^a = \sum_{m=-R/h_1}^{R/h_1-1} \sum_{q=1}^Q w_{q,m} \kappa_T^a(s_{q,m}) U(s_{q,m}) \psi_0, \quad I_{2,h}^a = \sum_{m=-R/h_1}^{R/h_1-1} \sum_{q=1}^Q w_{q,m} \Lambda_T^a(s_{q,m}) U(s_{q,m}) \mathbf{b}.$$

Then the total errors satisfy

$$\|I_{1,h}^a - I_1\| \lesssim \delta_{\text{off}} \|\psi_0\| + 2^{-2Q+1} \frac{R}{\sqrt{T}} \left( \frac{h_1}{\sqrt{T}} \right)^{2Q} \left( \|H\| + \frac{1}{\sqrt{2T}} \right)^{2Q} \|\psi_0\| + \frac{\sqrt{T}}{R} e^{-\frac{R^2}{4T}} \|\psi_0\|, \quad (\text{A.7})$$

$$\|I_{2,h}^a - I_2\| \lesssim \delta_{\text{off}} T \|\mathbf{b}\| + 2^{-2Q+1} R \sqrt{T} \left( \frac{h_1}{\sqrt{T}} \right)^{2Q} \left( \|H\| + \frac{1}{\sqrt{2T}} \right)^{2Q} \|\mathbf{b}\| + \frac{T \sqrt{T}}{R} e^{-\frac{R^2}{4T}} \|\mathbf{b}\|. \quad (\text{A.8})$$

*Proof.* We treat  $I_{1,h}^a$ ; the estimate for  $I_{2,h}^a$  is analogous. By the triangle inequality,

$$\|I_{1,h}^a - I_1\| \leq \|I_{1,h}^a - I_{1,h}\| + \|I_{1,h} - I_{1,\text{trunc}}^{(R)}\| + \|I_{1,\text{trunc}}^{(R)} - I_1\|.$$

Using (3.10) and  $\|U(s)\| = 1$ , one has

$$\|I_{1,h}^a - I_{1,h}\| \leq \sum_{m,q} w_{q,m} |\kappa_T^a(s_{q,m}) - \kappa_T(s_{q,m})| \|\psi_0\| \leq \delta_{\text{off}} \sum_{m,q} w_{q,m} \kappa_T(s_{q,m}) \|\psi_0\|.$$

Lemma A.3 implies  $\sum_{m,q} w_{q,m} \kappa_T(s_{q,m}) \lesssim 1$ , hence  $\|I_{1,h}^a - I_{1,h}\| \lesssim \delta_{\text{off}} \|\psi_0\|$ . Lemma A.1 bounds the quadrature error  $\|I_{1,h} - I_{1,\text{trunc}}^{(R)}\|$  and yields the middle term in (A.7). Lemma A.1 gives

$$\|I_{1,\text{trunc}}^{(R)} - I_1\| \leq \text{erfc} \left( \frac{R}{2\sqrt{T}} \right) \|\psi_0\| \leq \frac{\sqrt{T}}{R} e^{-R^2/(4T)} \|\psi_0\|,$$

which yields the last term in (A.7).

For  $I_{2,h}^a$ , the same decomposition together with (3.11), Lemmas A.3, A.2, and A.1 yields (A.8).  $\square$

**Acknowledgement** SJ acknowledges the support of the NSFC grant No. 12341104, the Shanghai Pilot Program for Basic Research, the Science and Technology Commission of Shanghai Municipality (STCSM) grant no. 24LZ1401200, the Shanghai Jiao Tong University 2030 Initiative, and the Fundamental Research Funds for the Central Universities. CM was partially supported by NSFC grant No. 12501607, and the Science and Technology Commission of Shanghai Municipality (No.22DZ2229014).

## References

- [1] D. An, A. W. Childs, and L. Lin. Quantum algorithm for linear non-unitary dynamics with near-optimal dependence on all parameters. *arXiv:2312.03916*, 2023.
- [2] D. An, D. Fang, and L. Lin. Time-dependent Hamiltonian simulation of highly oscillatory dynamics and superconvergence for Schrödinger equation. *Quantum*, 6:690, 2022.
- [3] D. An, J. Liu, and L. Lin. Linear combination of Hamiltonian simulation for non-unitary dynamics with optimal state preparation cost. *Phys. Rev. Lett.*, 131(15):150603, 2023.

- [4] D. W. Berry. High-order quantum algorithm for solving linear differential equations. *J. Phys. A: Math. Theor.*, 47(10):105301, 17 pp., 2014.
- [5] D. W. Berry, A. M. Childs, R. Cleve, R. Kothari, and R. D. Somma. Simulating Hamiltonian Dynamics with a truncated Taylor series. *Phys. Rev. Lett.*, 114(9), 2015.
- [6] D. W. Berry, A. M. Childs, R. Cleve, R. Kothari, and R. D. Somma. Exponential improvement in precision for simulating sparse Hamiltonians. *Forum of Mathematics, Sigma*, 5, 2017.
- [7] D. W. Berry, A. M. Childs, and R. Kothari. Hamiltonian simulation with nearly optimal dependence on all parameters. In *2015 IEEE 56th Annual Symposium on Foundations of Computer Science*, pages 792–809, 2015.
- [8] D. W. Berry, A. M. Childs, A. Ostrander, and G. Wang. Quantum algorithm for linear differential equations with exponentially improved dependence on precision. *Comm. Math. Phys.*, 356(3):1057–1081, 2017.
- [9] D. W. Berry and P. C. S. Costa. Quantum algorithm for time-dependent differential equations using Dyson series. *Quantum*, 8:1369, 2024.
- [10] R. W. Carroll and R. E. Showalter. *Singular and Degenerate Cauchy Problems*. Academic Press, New York, 1976.
- [11] S. Chakraborty, A. Gilyén, and S. Jeffery. The power of block-encoded matrix powers: Improved regression techniques via faster Hamiltonian simulation. In *Proceedings of the 46th International Colloquium on Automata, Languages, and Programming (ICALP 2019)*, 2019.
- [12] A. M. Childs, R. Kothari, and R. D. Somma. Quantum algorithm for systems of linear equations with exponentially improved dependence on precision. *SIAM J. Comput.*, 46(6):1920–1950, 2017.
- [13] A. W. Childs and J. Liu. Quantum spectral methods for differential equations. *Comm. Math. Phys.*, 375(2):1427–1457, 2020.
- [14] J. D. Cole. On a quasi-linear parabolic equation occurring in aerodynamics. *Quarterly of Applied Mathematics*, 9(3):225–236, 1951.
- [15] R. Courant and D. Hilbert. *Methods of Mathematical Physics*, volume II. John Wiley & Sons, New York, 1962.
- [16] D. Dong, Y. Li, and J. Xue. A quantum algorithm for linear autonomous differential equations via Padé approximation. *Quantum*, 9:1770, 2025.
- [17] D. Fang, L. Lin, and Y. Tong. Time-marching based quantum solvers for time-dependent linear differential equations. *Quantum*, 7:955, 2023.
- [18] A. Gilyén, Y. Su, G. H. Low, and N. . Quantum singular value transformation and beyond: exponential improvements for quantum matrix arithmetics. In *Proceedings of the 51st Annual ACM SIGACT Symposium on Theory of Computing*, pages 193–204, 2019.

[19] Diogo A. Gomes and Enrico Valdinoci. Entropy penalization methods for Hamilton–Jacobi equations. *Advances in Mathematics*, 215(1):94–152, 2007.

[20] R. Griego and R. Hersh. Theory of random evolutions with applications to partial differential equations. *Trans. Amer. Math. Soc.*, 156:405–418, 1971.

[21] A. W. Harrow, A. Hassidim, and S. Lloyd. Quantum algorithm for linear systems of equations. *Phys. Rev. Lett.*, 103(15):150502, 2009.

[22] R. Hersh. *The method of transmutations*. Lecture Notes in Mathematics. Springer, 1975.

[23] J. D. Hidary. *Quantum Computing: An Applied Approach*. Springer, 2019.

[24] E. Hopf. The partial differential equation  $u_t + uu_x = \mu u_{xx}$ . *Communications on Pure and Applied Mathematics*, 3(3):201–230, 1950.

[25] S. Jin and N. Liu. Quantum algorithms for viscosity solutions to nonlinear hamilton-jacobi equations based on an entropy penalisation method. *arXiv e-prints*, 2025.

[26] S. Jin, N. Liu, and C. Ma. On Schrödingerization based quantum algorithms for linear dynamical systems with inhomogeneous terms. *arXiv:2402.14696*, 2024.

[27] S. Jin, N. Liu, C. Ma, Y. Peng, and Y. Yu. On the schrödingerization method for linear non-unitary dynamics with optimal dependence on matrix queries. *arXiv:2505.00370*, 2025.

[28] S. Jin, N. Liu, and Y. Yu. Time complexity analysis of quantum difference methods for linear high dimensional and multiscale partial differential equations. *J. Comput. Phys.*, 471:111641, 2022.

[29] S. Jin, N. Liu, and Y. Yu. Quantum simulation of partial differential equations: Applications and detailed analysis. *Phys. Rev. A*, 108:032603, 2023.

[30] S. Jin, N. Liu, and Y. Yu. Quantum simulation of partial differential equations via schrödingerization. *Phys. Rev. Lett.*, 133:230602, 2024.

[31] Y. Kannai. Off diagonal short time asymptotics for fundamental solution of diffusion equation. *Communications in Partial Differential Equations*, 2(8):781–830, 1977.

[32] V. V. Katrakhov and S. M. Sitnik. A boundary–value problem for the steady–state schrödinger equation with a singular potential. *Dokl. Math.*, 30(2):468–470, 1984.

[33] M. Kieferová, A. Scherer, and D. W. Berry. Simulating the dynamics of time-dependent Hamiltonians with a truncated Dyson series. *Phys. Rev. A*, 99:042314, 13 pp., 2019.

[34] H. Krovi. Improved quantum algorithms for linear and nonlinear differential equations. *Quantum*, 7:913, 2023.

[35] X. Li. From linear differential equations to unitaries: A moment-matching dilation framework with near-optimal quantum algorithms. *arXiv:2507.10285*, 2025.

[36] L. Lin. Lecture notes on quantum algorithms for scientific computation. *arXiv:2201.08309*, 2022.

[37] J.-L. Lions. Opérateurs de delsarte et problèmes mixtes. *Bull. Soc. Math. France*, 81:9–95, 1956.

[38] J.-L. Lions. On the generalized radiation problem of weinstein. *J. Math. Mech.*, 8:873–888, 1959.

[39] G. H Low and I. L. Chuang. Optimal Hamiltonian simulation by quantum signal processing. *Phys. Rev. Lett.*, 118(1), 2017.

[40] G. H. Low and I. L. Chuang. Hamiltonian simulation by qubitization. *Quantum*, 3:163, 2019.

[41] G. H. Low and R. D. Somma. Optimal quantum simulation of linear non-unitary dynamics. *arXiv:2508.19238*, 2025.

[42] G. H. Low and N. Wiebe. Hamiltonian simulation in the interaction picture. *arXiv:1805.00675v2*, 2019.

[43] Qi Lü and Enrique Zuazua. Averaged controllability for random evolution partial differential equations. *J. Math. Pures Appl.*, 105(3):367–414, 2016.

[44] M. A. Nielsen and I. L. Chuang. *Quantum Computation and Quantum Information*. Cambridge, New York, 2010.

[45] J. Preskill. Quantum computing in the NISQ era and beyond. *Quantum*, 2:79, 2018.

[46] E. G. Rieffel and W. H. Polak. *Quantum Computing: A Gentle Introduction*. MIT Press, 2011.

[47] R. L. Schilling, R. Song, and Z. Vondraček. *Bernstein Functions: Theory and Applications*. De Gruyter, 2 edition, 2012.

[48] Z. X. Shang, N. Guo, D. An, and Q. Zhao. Designing a nearly optimal quantum algorithm for linear differential equations via lindbladians. *Physical Review Letters*, 135(12):120604, 2025.

[49] S. M. Sitnik. Transmutations and applications: A survey. *arXiv e-prints*, 2012. arXiv:1012.3741v1.

[50] Y. Subaşı, R. D. Somma, and D. Orsucci. Quantum algorithms for systems of linear equations inspired by adiabatic quantum computing. *Phys. Rev. Lett.*, 122(6):060504, 2019.

[51] C. Wang, H. Y. Liu, C. Xue, X. N. Zhuang, M. Dou, Z. Y. Chen, and G. P. Guo. Quantum simulation of non-unitary dynamics via contour-based matrix decomposition. *arXiv:2511.10267*, 2025.

[52] H. C. Wu and X. Li. Structure-preserving quantum algorithms for linear and nonlinear Hamiltonian systems. *arXiv:2411.03599*, 2024.

- [53] G. Yang, A. Onwunta, and D. An. Quantum differential equation solvers with low state preparation cost: Eliminating the time dependence in dissipative equations. *arXiv:2508.15170*, 2025.
- [54] E. Zuazua. Control and numerics: Heat and waves. Lecture notes, FAU Erlangen–Nürnberg, 2020.